International Journal of Innovation Engineering and Science Research

Editorial Board

International Journal of Innovation Engineering and Science Research

Volume 3 ISSUE 2 March-April 2019

INFLUENCE OF PROCESSING MODES ON WEAR RESISTANCE OF COPPER AND GRAPHITE ELECTRODES

Yuriy Orlov || Denis Chemezov || Irina Medvedeva || Andrey Komissarov || Dmitriy Orlov || Margarita Bakhmeteva || Irina Pavluhina

Study of The dynamics of rotor-bearing using MATLAB and finite elements

Brihmat Mostefa || Refassi Kaddour || Douroum Embarek

To the question of a process optimization of cast in a metal mould of automotive pistons made of grey cast iron and silumin

Denis Chemezov || Irina Medvedeva || Alexandra Strunina || Tatyana Komarova || Ivan Mochalov || Polina Nikitina

MANETs in Military Communications Design Concepts and Challenges

Dalal Alshammari || Salman Al-Shehri

International Journal of Innovation Engineering and Science Research
(ISSN: 2581-4591)
www.ijiesr.com

INFLUENCE OF PROCESSING MODES ON WEAR RESISTANCE OF COPPER AND GRAPHITE ELECTRODES

Yuriy Orlov[1], Denis Chemezov[2], Irina Medvedeva[2], Andrey Komissarov[2], Dmitriy Orlov[1], Margarita Bakhmeteva[2], Irina Pavluhina[2]

[1]Vladimir State University named after Alexander and Nikolay Stoletovs
[2]Vladimir Industrial College
Vladimir, Russian Federation

ABSTRACT

Wear resistance of electrodes in dependence on materials from which they are made and modes of electrical discharge machining is researched in the experiment.

Keywords *– an electrode, electrical discharge machining, wear.*

I. INTRODUCTION

Replacement of traditional methods of mechanical processing of the machine parts to physic-chemical processing methods (without the use of cutting edge tools) is due to the use in engineering of metallic alloys possessing by the special properties (heat-resistant steels, cemented carbides, tool steels and etc.), high accuracy of mating surfaces and complex configuration of the parts. These technical requirements are observed in conditions of electrical discharge machining (EDM) of the part. EDM of the part is performed by an electrode which is made of conductive materials [1]. The EDM process is the destruction of the workpiece material under the action of electrical discharges occurring between the workpiece and the electrode. The destruction of the electrode leads to a change of its initial sizes (absolute wear). Intensity of electrode wear depends on the modes of EDM and tool material [2; 3; 4]. Wear resistance of the electrode is determined only approximately due to the complexity of the wear process. The research of wear resistance of the electrodes in dependence on materials from which they are made and modes of EDM will allow to select a tool which is provided the highest machining productivity, high dimensional accuracy and surfaces quality of the part.

II. MATERIAL AND METHOD

For performing of the experiment 6 tool-electrodes was made: 3 copper electrodes (copper 1108, copper 1107 and copper 1106) and 3 graphite electrodes (graphite 3108, graphite 3107 and graphite 3106). The outer diameter of the working part of all the electrodes is 6 mm. Configuration of the electrodes is presented in the Fig. 1.

Fig. 1. Copper and graphite electrodes before EDM.

Die tool steel X37CrMoV5-1 (EN) was used as processed material. This steel is often used in the manufacture of working parts of moulds for pressure casting. Before EDM the workpiece of this steel was exposed by heat treatment to hardness 45...48 HRC and was grinded with both sides.
EDM of 6 blind holes by the copper and graphite electrodes was performed on the electric discharge machine Mondo Star 20 (Elox Corporation, USA). General view of the electric discharge machine and its technical parameters are presented in the Fig. 2 and in the table 1, respectively.

Fig. 2. The electric discharge machine Mondo Star 20.

TABLE I. THE TECHNICAL PARAMETERS OF THE ELECTRIC DISCHARGE MACHINE MONDO STAR 20.

External dimensions (width × depth × height)	
1550×1130×2360 mm	
Operating weight	
1580 kg	
Connection	
Operating power consumption	9.9 KVA
Maximum current consumption	15 A
Mains voltage	3×400V, 50/60 Hz
Mains quality	± 10 % (IEC 38) without interruption
Cos, φ	> 8
Water connection / temperature / water quantity / pressure	Ø 16 mm / Ambient temperature – 7 °C / 15 lpm / 2 – 7 Bar

Exhauster connection	Ø 100 mm
Maximum sizes of workpiece (width × depth × height)	
630×400×165 mm	
Working part of table (length × width)	
400×300 mm	
X-Y-Z range	
300/250/250 mm	
Movable sleeve (min/max)	
188/438 mm	
Maximum weight of workpiece	
200 kg	
Maximum weight of electrode	
25 kg	
Actuator	
Axes X/Y/Z	DC – servomotor
Minimum programmable movement	0.001 mm
Movement speed	720 mm/min
Accuracy	
VDI 3441 [5]	
Positioning error (Z) Pa	0.01/250
Positioning error (X, Y) Pa	0.01/300
Average range of positioning variations Ps	0.003 mm
Average error of reverse motion U	0.003 mm
Remote control (setup function)	
Standard	
Flushing	
Number of channels flushing	3
Pressure flushing and automatic pulse pressure flushing	2
Flushing by suction	1
Connection of programmable flushing	1
DA-dielectric assembly	
Type	Embedded
Fill volume	300 l
Type of used filters	Paper (cartridge filters)
Autonomous operation of filters	30 hours at 30 A
C-axis for indexing, rotation and erosion in a spiral	
Maximum weight of electrodes	25 kg
Maximum permissible current	60 A
Maximum number of turns	0 – 55 RPM
Positioning error Pa	0.01°
Average range of positioning variations Ps	0.005°
Average error of reverse motion U	0.005°
ELM – electrodes magazine (option)	
Number of electrodes	4 to the right
Maximum sizes of electrode (length × width × height)	70/80/165 mm
Maximum weight of all electrodes in magazine	9 kg
Air pressure	7 Bar
Futura V	
Generator / control / user shell	
Generator	
Maximum operating current	64 A
Number of channels	1
Removal rate according to values AGIE	

Vw Cu / St	380 mm^3/min at 64 A
Vw Gr / St	500 mm^3/min at 64 A
Environment requirements	
20 °C / temperature changes ≤ 0.5 °C per hour, ≤ 2 °C per day / without vibrations, draughts and heat sources	

For the experiment there were taken three modes of EDM (rough machining, semi-finish machining and finish machining) which are differ by feed rate, accuracy and quality. Modes of EDM of holes by the copper and graphite electrodes are presented in the table 2.

TABLE II. MODES OF EDM.

Rough machining			
Electrode material	*Voltage U, V*	*Current strength I, A*	*Power current P*
Copper 1108	100	8	3
Graphite 3108	100	8	8
Semi-finish machining			
Electrode material	*Voltage U, V*	*Current strength I, A*	*Power current P*
Copper 1107	100	7	2
Graphite 3107	100	7	8
Finish machining			
Electrode material	*Voltage U, V*	*Current strength I, A*	*Power current P*
Copper 1106	100	6	2
Graphite 3106	100	6	6

Machining within an hour with two breaks for measuring of depth of the processed hole and wear of the tool was carried out by the each electrode.

III. RESULT AND DISCUSSION

The results of the performed experiment are presented by the dependencies of EDM rates of the holes by the copper and graphite electrodes from the adopted modes (the Fig. 3 A – 8 A). The dependencies of wear of the copper and graphite electrodes from depth and time of EDM are presented in the Fig. 3 B, C – 8 B, C.

Rate of EDM of the hole by the copper electrode (rough machining) was amounted to 7.43 mm/h. The dependence of depth of EDM from time is close to linear. Rate of electrode wear is gradually increased. The surfaces smoothness of the hole and machining accuracy are low. For the accuracy in this case is taken that how insofar the processed surface coincides with geometry of the electrode before machining.

Rate of EDM of the hole during semi-finish machining by the copper electrode was amounted to 4.21 mm/h. The dependence of depth of EDM from time is close to linear.

Rate of EDM of the hole during finish machining by the copper electrode was amounted to 1 mm/h. Rate of electrode wear from time of EDM is reduced. This is due to the accelerated burning of asperity of the electrode surface and the gradual change of geometry of the end surface of the tool (to the full machining area). The surfaces smoothness of the hole and machining accuracy are high.

Rate of EDM of the hole during rough machining by the graphite electrode was amounted to 8.23 mm/h. The dependence of depth of EDM from time is close to linear, and rate of electrode wear is gradually reduced.

Rates of EDM of the holes during semi-finish and finish machining by the graphite electrodes were amounted to 2.54 mm/h and 1.34 mm/h respectively. When finish machining it is achieved only high accuracy of the hole.

Wear u of the copper electrode 1108 from time t and depth h of EDM of the workpiece material can be presented by the following equations (1):

$$\begin{cases} u = 0.0031t^{0.8145} \\ u = 0.0093h^{1.1144} \end{cases} \quad (1)$$

Wear of the copper electrode 1107 from time and depth of EDM of the workpiece material can be presented by the following equations (2):

$$\begin{cases} u = 0.0038t^{0.6818} \\ u = 0.0253h^{0.6272} \end{cases} \quad (2)$$

Wear of the copper electrode 1106 from time and depth of EDM of the workpiece material can be presented by the following equations (3):

$$\begin{cases} u = 0.0001t^{1.3382} \\ u = 0.0281h^{1.2182} \end{cases} \quad (3)$$

Wear of the graphite electrode 3108 from time and depth of EDM of the workpiece material can be presented by the following equations (4):

$$\begin{cases} u = 0.0014t^{1.2352} \\ u = 0.0054h^{1.7679} \end{cases} \quad (4)$$

Wear of the graphite electrode 3107 from time and depth of EDM of the workpiece material can be presented by the following equations (5):

$$\begin{cases} u = 0.0021t^{0.8851} \\ u = 0.0414h^{0.6793} \end{cases} \quad (5)$$

Wear of the graphite electrode 3106 from time and depth of EDM of the workpiece material can be presented by the following equations (6):

$$\begin{cases} u = 7\times10^{-5}t^{1.2576} \\ u = 0.0087h^{1.1509} \end{cases} \quad (6)$$

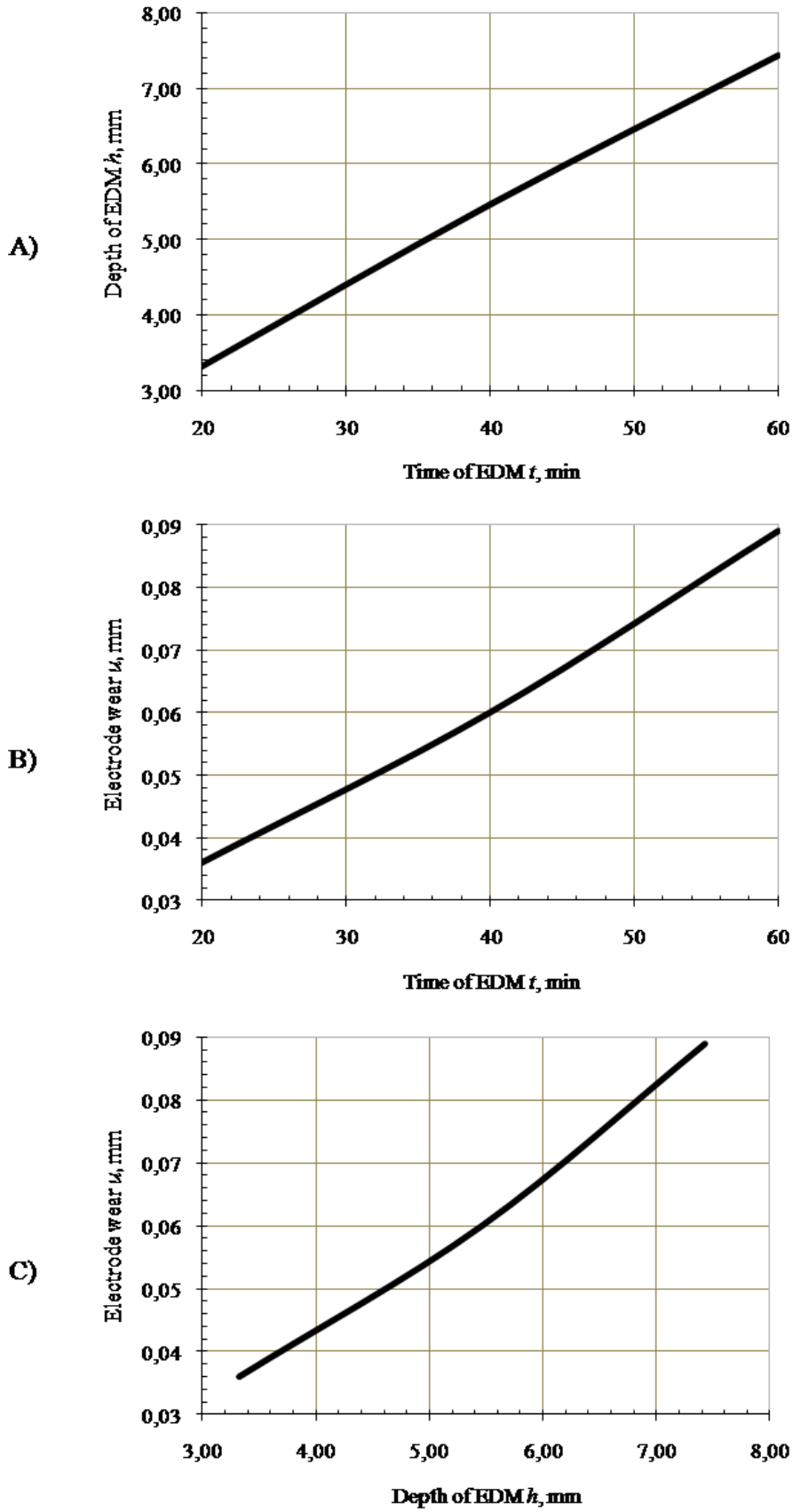

Fig. 3. Rough EDM of material by the copper electrode 1108: A – the dependence of depth of EDM from time of EDM, B – the dependence of electrode wear from time of EDM, C – the dependence of electrode wear from depth of EDM.

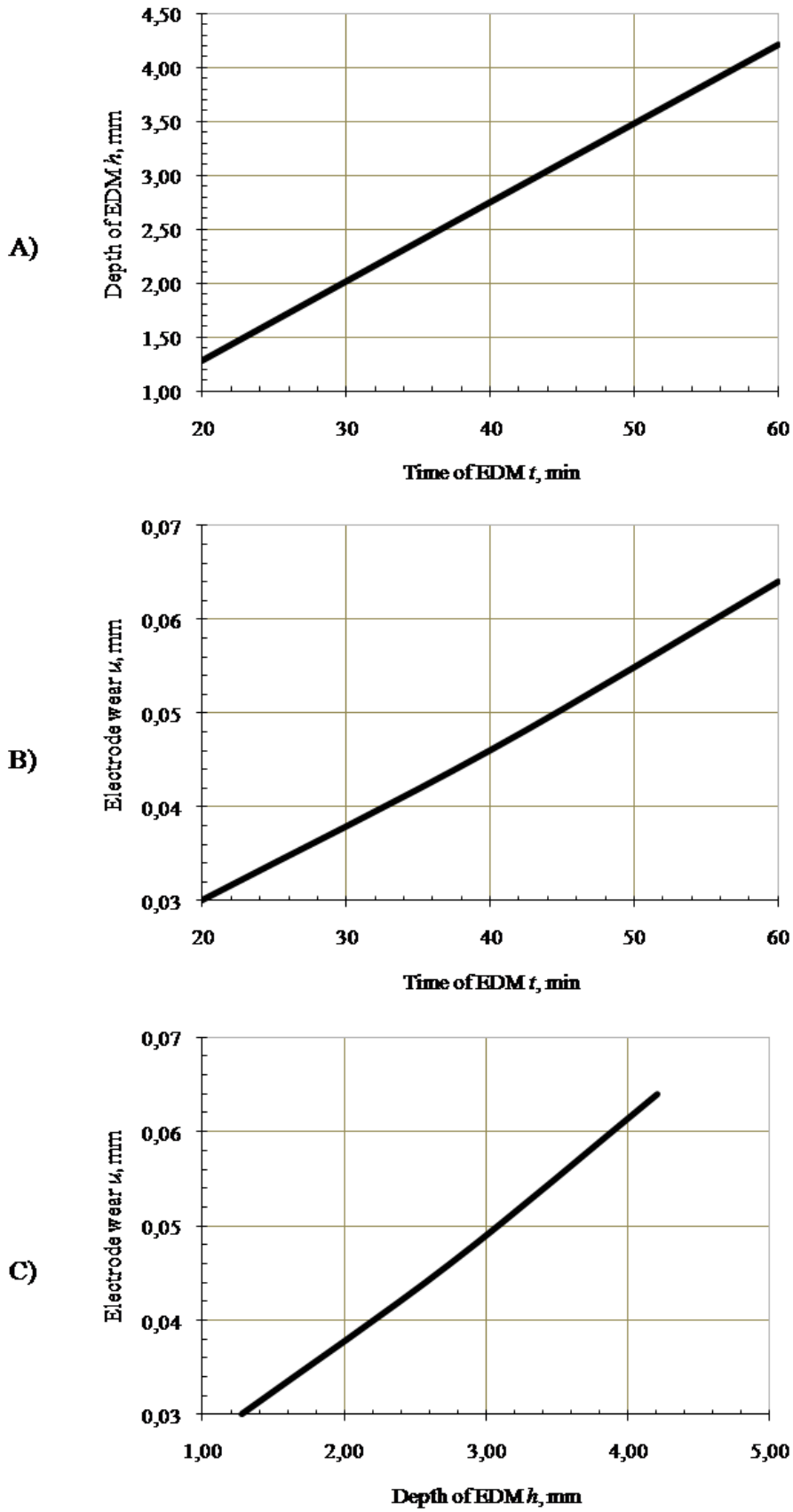

Fig. 4. Semi-finish EDM of material by the copper electrode 1107: A – the dependence of depth of EDM from time of EDM, B – the dependence of electrode wear from time of EDM, C – the dependence of electrode wear from depth of EDM.

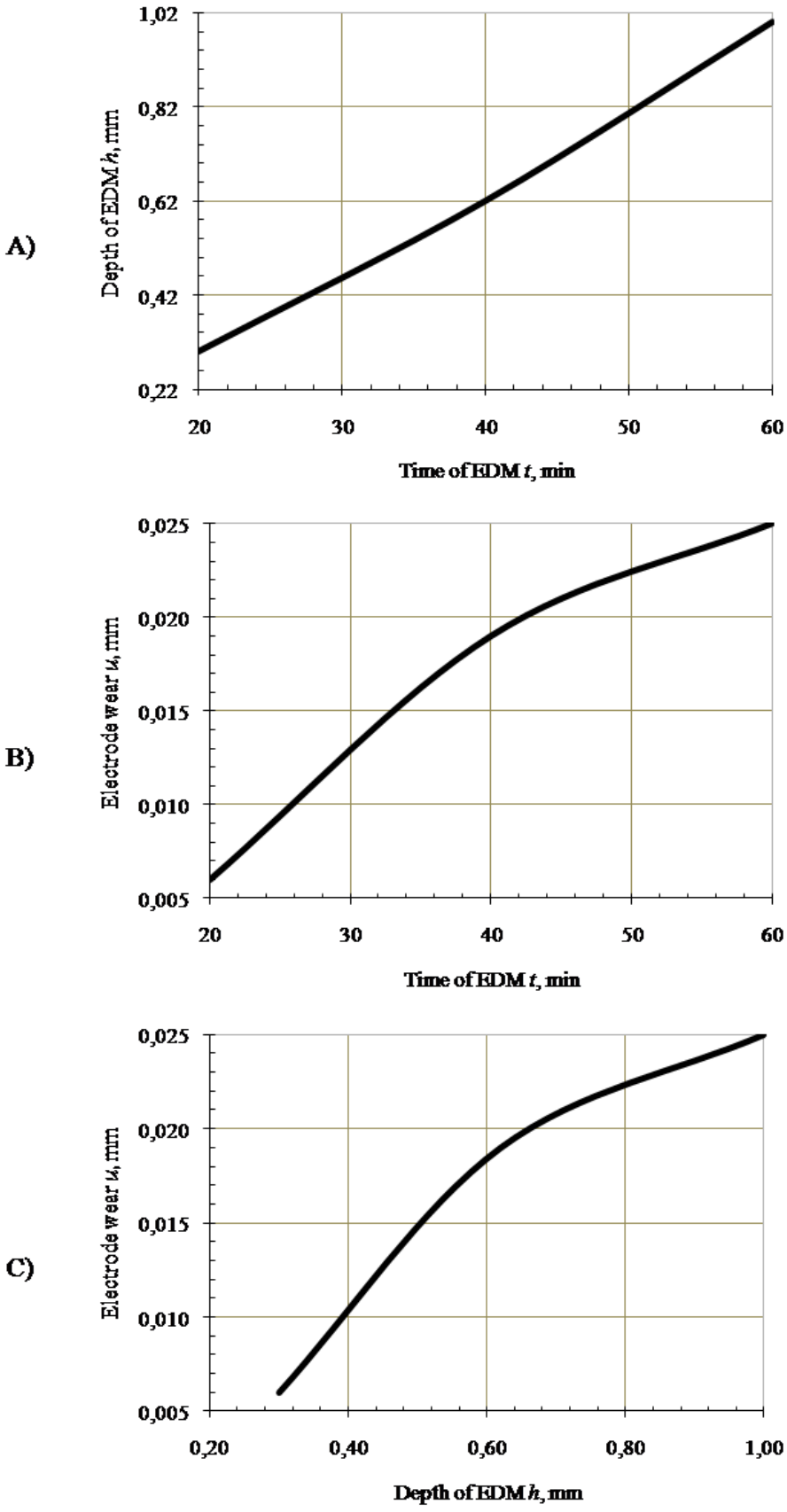

Fig. 5. Finish EDM of material by the copper electrode 1106: A – the dependence of depth of EDM from time of EDM, B – the dependence of electrode wear from time of EDM, C – the dependence of electrode wear from depth of EDM.

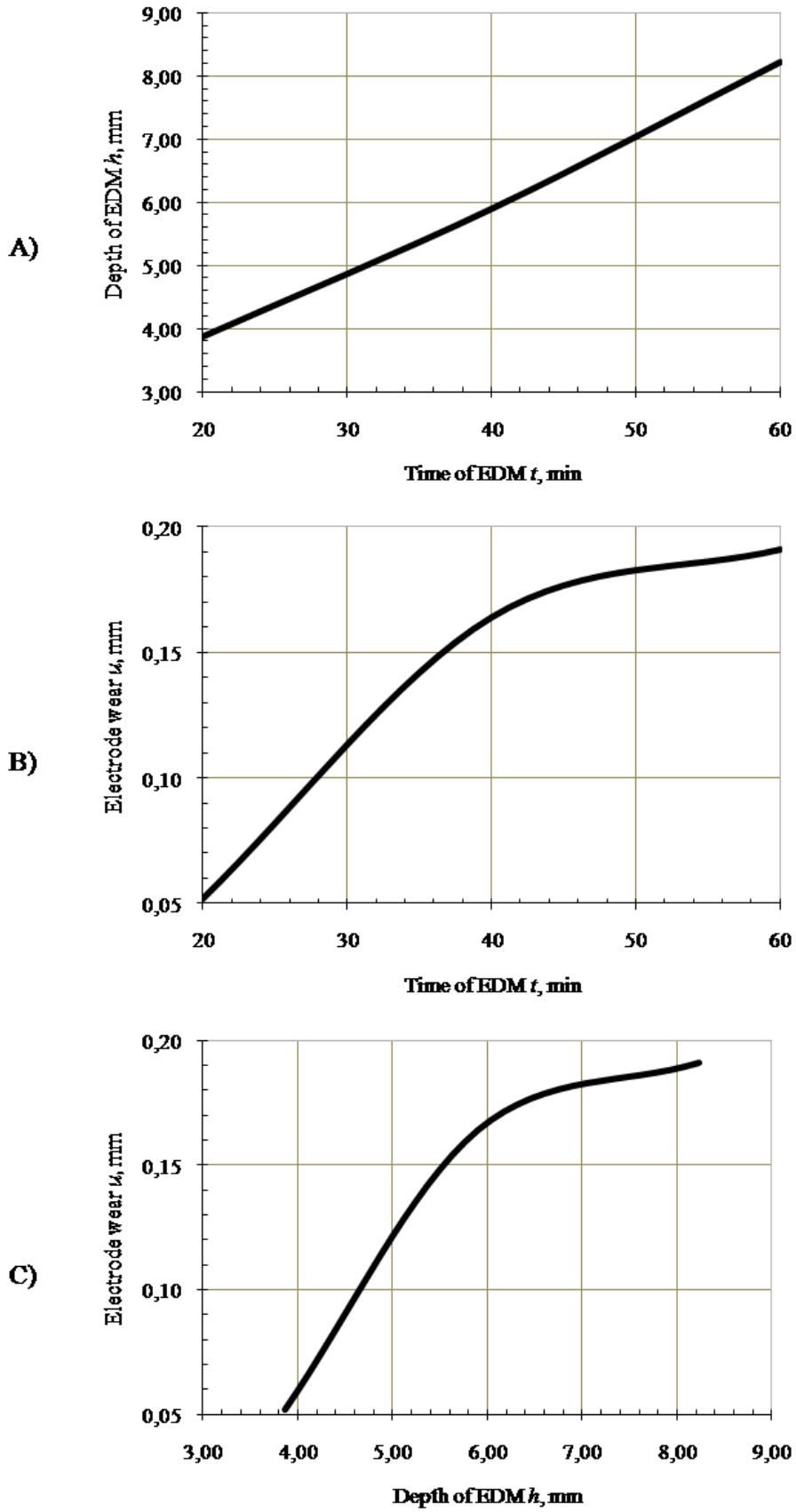

Fig. 6. Rough EDM of material by the graphite electrode 3108: A – the dependence of depth of EDM from time of EDM, B – the dependence of electrode wear from time of EDM, C – the dependence of electrode wear from depth of EDM.

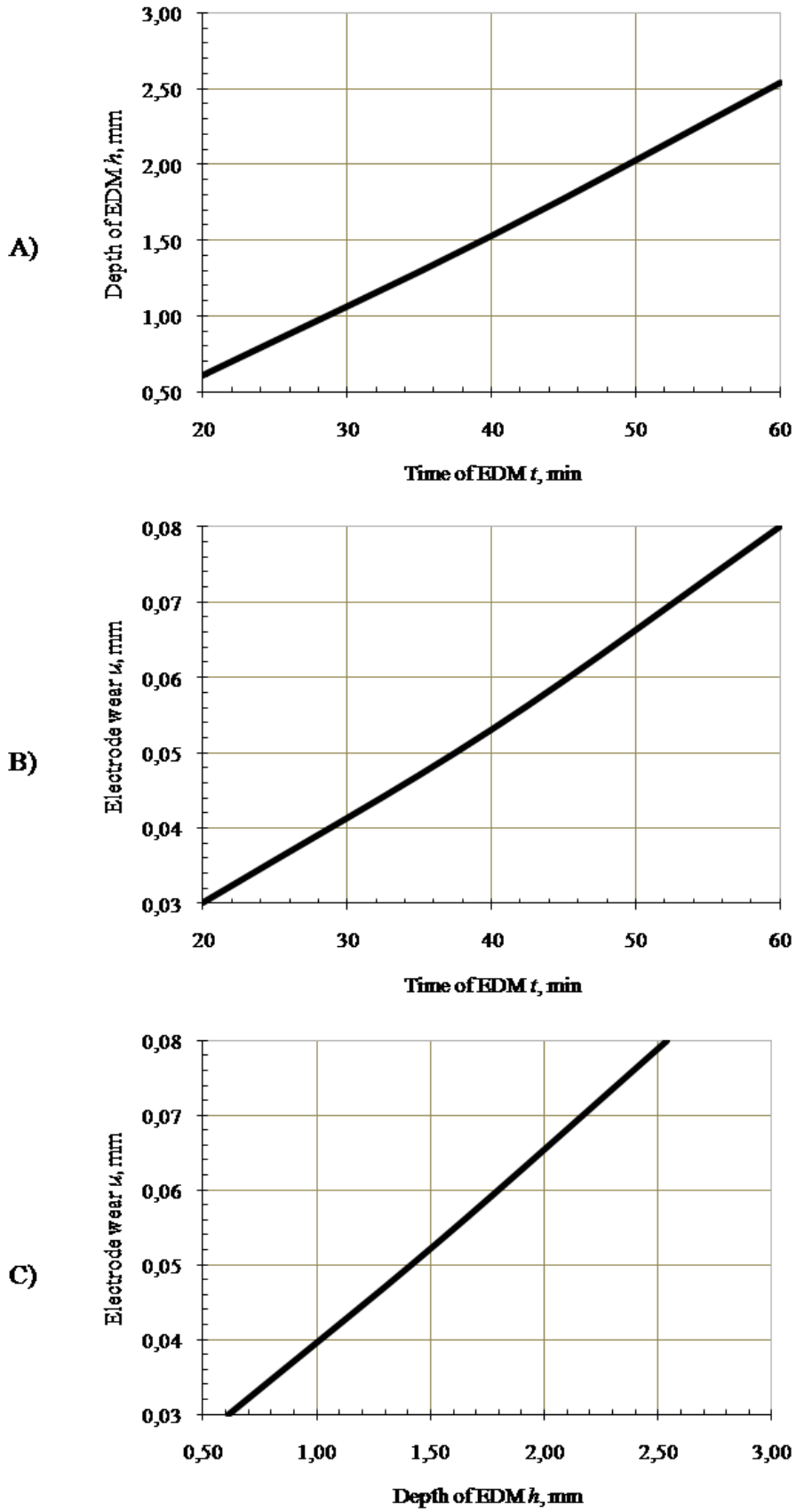

Fig. 7. Semi-finish EDM of material by the graphite electrode 3107: A – the dependence of depth of EDM from time of EDM, B – the dependence of electrode wear from time of EDM, C – the dependence of electrode wear from depth of EDM.

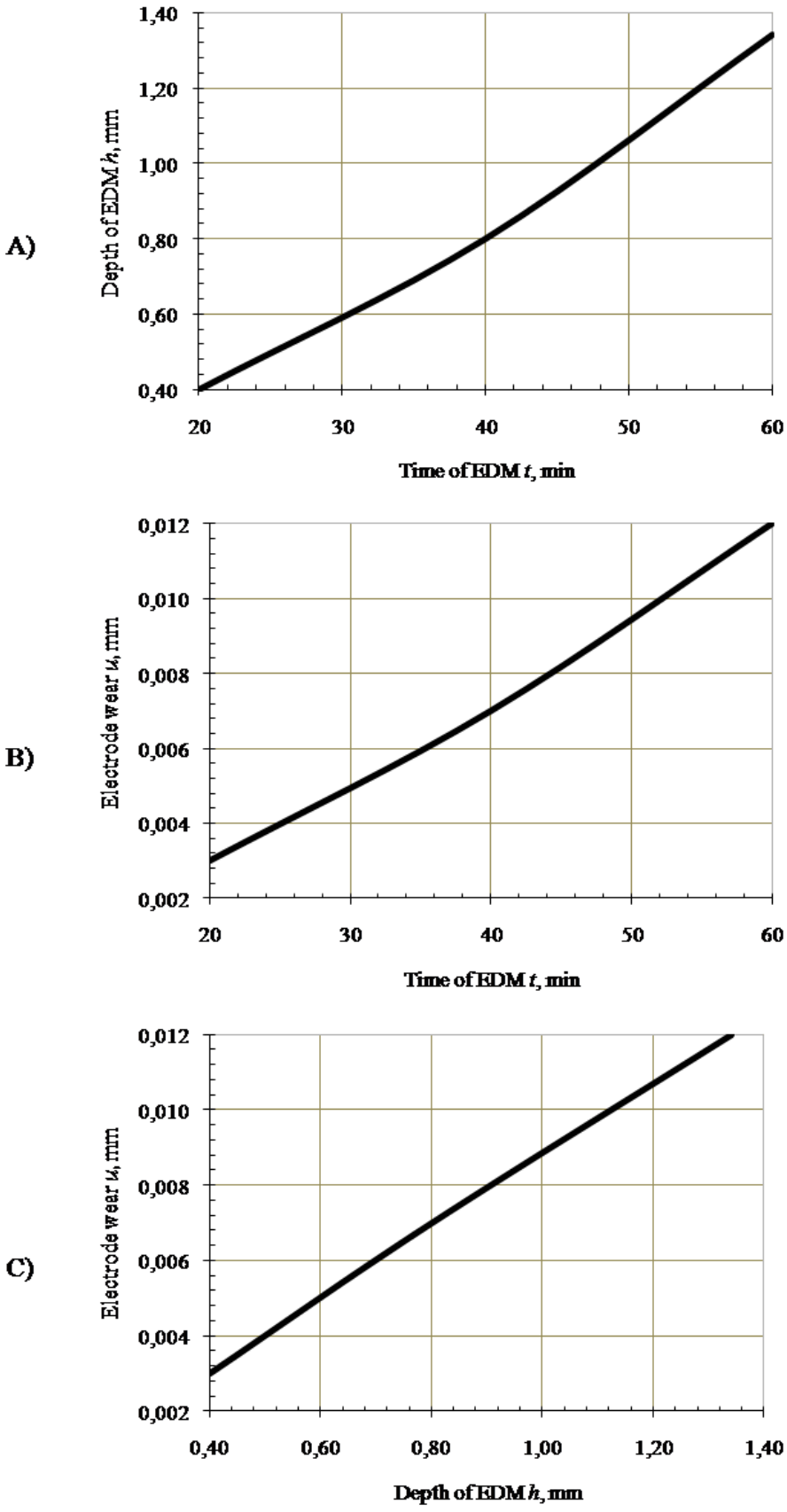

Fig. 8. Finish EDM of material by the graphite electrode 3106: A – the dependence of depth of EDM from time of EDM, B – the dependence of electrode wear from time of EDM, C – the dependence of electrode wear from depth of EDM.

Wear of the copper and graphite electrodes after EDM of the holes is presented in the Fig. 9 and 10. Surfaces quality of the holes after EDM is presented in the Fig. 11.

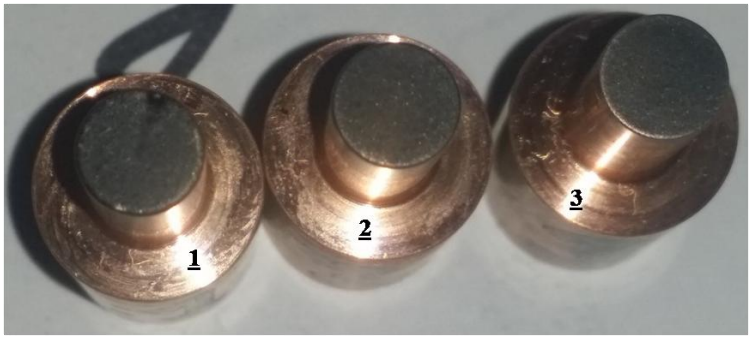

Fig. 9. Wear of the copper electrodes after EDM: 1 – copper 1108 (rough machining), 2 – copper 1107 (semi-finish machining), 3 – copper 1106 (finish machining).

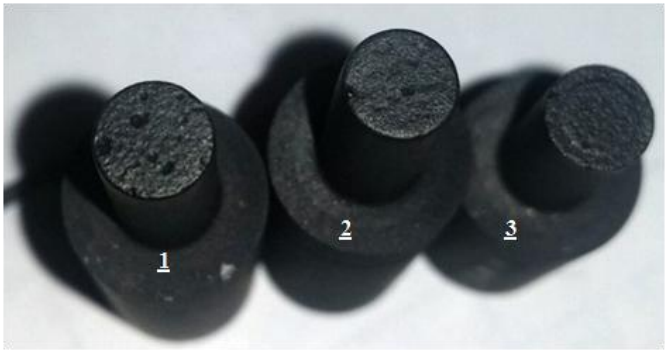

Fig. 10. Wear of the graphite electrodes after EDM: 1 – graphite 3108 (rough machining), 2 – graphite 3107 (semi-finish machining), 3 – graphite 3106 (finish machining).

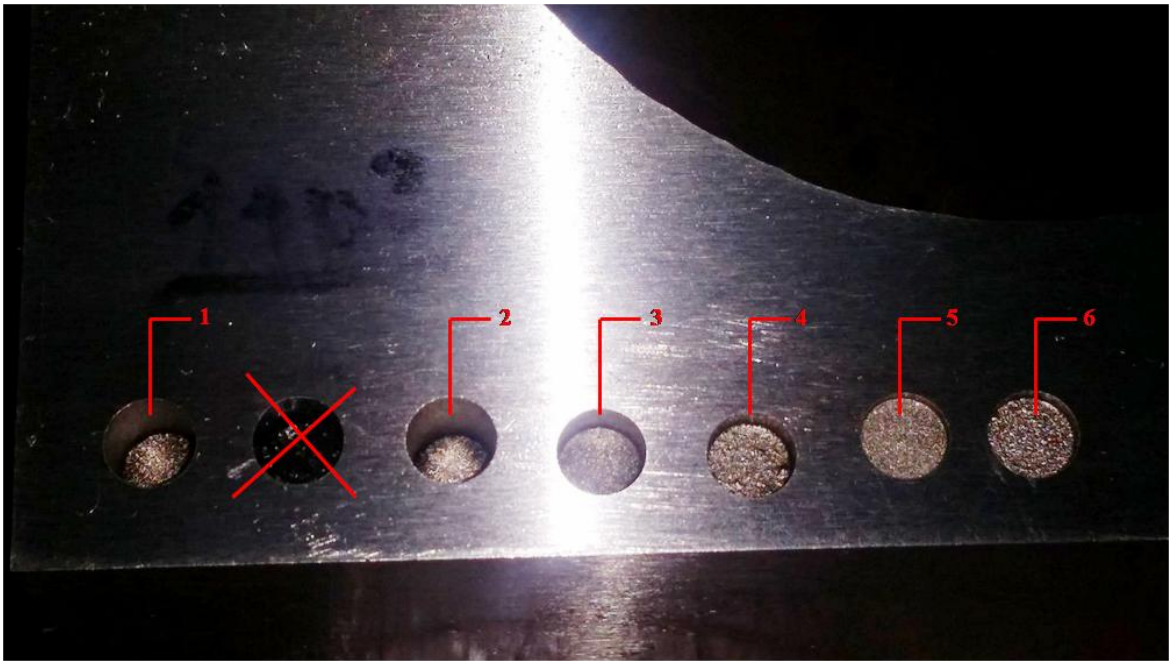

Fig. 11. Surface quality of the holes after EDM: 1 – machining by the copper electrode 1108, 2 – machining by the graphite electrode 3108, 3 – machining by the copper electrode 1107, 4 – machining by the graphite electrode 3107, 5 – machining by the copper electrode 1106, 6 – machining by the graphite electrode 3106.

IV. Conclusion

Wear resistance of the electrodes during EDM is depended on the tool material, machining modes and the volume of processed material.

It is determined that when rough machining the graphite electrode is used more effective. For equal amount of time the graphite electrode has been removed more material than the copper electrode (8.23 mm vs. 7.43 mm). Herewith, the greatest absolute wear was defined for the graphite electrode (0.191 mm vs. 0.089 mm). The copper electrode should be applied when semi-finish machining. When finish machining the graphite electrode has been removed 30 % more material than the copper electrode, but a roughness class of the processed surface of the hole is turned out below. In conditions of finish machining, wear resistance of working part of the graphite electrode in two times more than wear resistance of working part of the copper electrode.

The selection of the aforementioned parameters should be performed based on the technical specifications on manufacture of the part, such as dimensional accuracy, surface roughness, processability. For machining of working parts of the mould with high requirements to dimensional accuracy and surfaces roughness, it is necessary to use the copper electrodes in finishing modes. Technical requirements for the part manufacturing in this case are provided, but productivity of EDM is reduced (1 mm/h). In this case, it is economically advantageous to make two electrodes: one is graphite for rough machining with an allowance and one is copper for finish machining. Thereby, time of EDM of the main volume of the workpiece material will be reduced in 8.2 times.

References

[1] Complete EDM handbook. *Ram EDM electrodes and finishing, part 11*, 155 – 169.

[2] Aghdeab, S. H., Mahdi AL-Tameemi, W. I., & Jawad, A. F. (2014). Study the Effect of Electrode Wear Weight (EWW) in Electrical Discharge Machining (EDM). *Eng. & Tech. Journal, Vol. 32, part A, No. 6*, 1433 – 1441.

[3] Tirla, A., Popa, M. S., Pop, G. M., Chetreanu-Don, C. O., Oltean, A. I., & Preja, D. (2010). An electrode wear compensation model regarding the EDM process. *Annals of DAAAM for 2010 & proceedings of the 21st International DAAAM Symposium, Volume 21, No. 1*.

[4] Arthur, A., Dickens, Ph., Bocking, C., & Cobb, R. (1996). Wear & failure mechanisms for SL EDM electrodes. *Annual International Solid Freeform Fabrication Symposium*, 175 – 190.

[5] VDI/DGQ 3441-1977. *Statistical Testing of the Operational and Positional Accuracy of Machine Tools. Basis*.

Study of The dynamics of rotor-bearing using MATLAB and finite elements

Brihmat Mostefa [1],Refassi Kaddour[1],Douroum Embarek [2]

[1]Laboratory of Mechanics of Structures and Solids.
University of djillali liabes Sidi bel abbes
22000, Algeria

[2]Laboratory of materials and reactive Systems.
University of sidi bel abbes 22000, Algeria

ABSTRACT

The dynamics of the rotors and the stability of the rotating machines, It plays an important role in improving the security and performance of these systems.
Two phenomena in rotor dynamics are particularly dangerous and can lead to unacceptable vibration levels, These are critical rotational speeds and linearly unstable regimes, the consequences of which are often catastrophic.The internal material damping in the rotor shaft introduces rotary dissipative forces which are proportional to spin speed and acts tangential to the rotor orbit. These forces influence the dynamic behaviour of a rotor and tend to destabilize the rotor shaft system as spin speed increases.So, In this paper in the study of the dynamic behavior of rotors, we are interested in:

- study of Hydrodynamic bearing effect on the rotor dynamics.
- Determination of the eigenvalues of the rotor as a function of its rotational speed and diagrams of : Campbell, stability, constant damping....

Keywords:dynamics, rotor, stability, critical rotational speeds, gyroscopic forces.

I. INTRODUCTION

Vibration control of turbo machinery is very important for the integrity of industrial plants. In this regard it is very important to predict the dynamic behavior of rotating machinery which operates above the first critical speed accurately. In fact, rotating motion and critical speeds are design criteria of rotating machinery and play an important role in diagnosis and control of rotors.
Harmonic response analysis is a technique used to determine the steady-state response of a linear structure to loads that vary sinusoidally (harmonically) with time and is used to predict the sustained dynamic behavior of structures to consistent cyclic loading. Thus, it can be verified whether or not a machine design will successfully overcome resonance, fatigue, and other harmful effects of forced vibrationsresponses, the influence of asymmetry can be analyzed using a Jeffott model with orthotropic bearings. It is shown (On unbalanced Genta [1], Childs [2]) that at low rotational speeds, the rotor is in direct precession. In the neighborhood and beyond the first critical speed, the behavior becomes retrograde type before becoming direct again for rotational speeds higher than the second critical speed. In comparison with a rotor with isotropic supports, where the orbits are circular for all the rotation frequencies, an anisotropic carrier rotor generates elliptical orbits. The shaft then undergoes normal axial stresses that affect the life of the machine. Also, rotors with anisotropic supports can be used to increase the frequency where instability occurs. Childs [2] shows, for example, that the instabilit originating in the internal damping is shifted thanks to the dissymmetry of the supports. Another phenomenon related to the anisotropy of the supports is the simultaneous manifestation of direct and retrograde precessions along the tree. Muszinska [3] has experimentally observed simultaneous precessions on a vertical rotor whose shaft is flexed. In this study, the

manifestation of simultaneous precessions is affected by the amplitude of the bending of the tree and also by the distribution of imbalances. Identical results (Dias et al [4]) were obtained for a horizontal rotor supported by bearings and bearings. These studies were confirmed by numerical simulations. Similarly, Rao et al. [5], [6] studied experimentally and numerically a horizontal Jeffcott rotor supported by two identical hydrodynamic bearings, showing that the variation of the radial clearance of the bearings (the parameter that controls the anisotropy) is the variable that drives the manifestation of simultaneous precessions: they then observe retrograde precession at the disk level and direct precession elsewhere. Finally,some Rotating machines may exhibit rotor asymmetry. These are, for example, two-pole generators or two-blade propeller systems.

The study of this type of rotor has attracted the attention of several researchers (Sakata et al [7], Kang et al [8], Genta [9]), who showed that this type of system generates a very dynamic rich whose characteristic phenomenon is the existence of a secondary critical speed. This critical speed appears at a speed close to half the synchronous critical speed, more precisely at the intersection of the direct mode frequency evolution curve with the excitation line f = 2F. This is then excited by a constant lateral force, such as the weight of the rotor. From a point of view of the appearance or not of instability, the rotating anisotropies bring up unstable frequency ranges which can be eliminated by the addition of external damping (Genta)[9].
Taplak [10] in his paper studied a program named Dynrot was used to make dynamic analysis and the evaluation of the results. For this purpose, a gas turbine rotor with certain geometrical and mechanical properties was modeled and its dynamic analysis was made by Dynrot program. Gurudatta [11] in his paper presented an alternative procedure called harmonic analysis to identify frequency of a system through amplitude and phase angle plots. The unbalance that exists in any rotor due to eccentricity has been used as excitation to perform such an analysis. ANSYS parametric design language has been implemented to achieve the results.

Sinou[12] investigated the response of a rotor's non- linear dynamics which is supported by roller bearings. He studies on a system comprised of a disk with a single shaft, two flexible bearing supports and a roller bearing. He found that the reason of the exciter is imbalance. He used a numerical method named Harmonic Balance Method for this study. Chouskey[13] et.al studied the influences of internal rotor material damping and the fluid film forces (generated as a result of hydrodynamic action in journal bearings) on the modal behavior of a flexible rotor-shaft system. It is seen that correct estimation of internal friction, in general, and the journal bearing coefficients at the rotor spin-speed are essential to accurately predict the rotor dynamic behaviour. This serves as a first step to get an idea about dynamic rotor stress and, as a result, a dynamic design of rotors.

Whalley and Abdul-Ameer[14], calculated the rotor resonance, critical speed and rotational frequency of a shaft that its, diameter changes by the length, by using basic harmonic response method.

Gasch[15], investigated the dynamic behavior of a Laval (Jeffcott) rotor with a transverse crack on its elastic shaft, and developed the non-linear motion equations which gave important clues on the crack diagnosis.

Das et al [16]. aimed to develop an active vibration control scheme to control the transverse vibrations on the rotor shaft arising from imbalance and they performed an analysis on the vibration control and stability of a rotor- shaft system which has electromagnetic exciters.

Villa et al. [17] studied the non-linear dynamic analysis of a flexible imbalanced rotor supported by roller bearings. They used Harmonic Balance Method for this purpose. Stability of the system was analyzed in frequency term with a method based on complexity. They showed that Harmonic Balance Method has realized the AFT strategy and harmonic solution very efficiently. Lei and Palazzolo [18] have analyzed a flexible rotor system supported by active magnetic bearings and synthesized the Campbell diagrams, case forms and eigen values to optimize the rotor-dynamic characteristics and obtained the stability at the speed range. They also investigated the rotor critical speed, case forms, frequency responses and time responses.

In addition, Łukasz Breńkacz et al. [19] described experimental research. Displacement signals were shown in the bearings and excitation forces used to determine the dynamics of the carrier. The study discussed in this article deals with the rotor supported by two hydrodynamic actuators working in a nonlinear manner. On the basis of calculations, dynamic transaction results were presented for a specific speed.
Fulaj et al. [20] discusses in his research how to obtain critical speeds of the rotor carrier system. A mathematical model for the flexible column was developed with a steel rotor using a specific element Techniques. The limited element model was used to obtain critical speeds in MATLAB.
This paper introduces an alternative procedure called harmonic analysis to determine the frequency of the system through critical speed using MATLAB. The language of matlab parameters design has been implemented to achieve results.
The basic studies of rotary dynamics are related to the Campbell scheme, which represents the evolution of self-repetition as a function of spin velocity and the calculation of unbalance responses mainly during the passage of critical velocity. In using the finite element method, we have seen that gyroscopic moments responsible for the variation of the natural frequency as a function of the speed of rotation or of the circulatory forces which make the movement unstable from a certain speed in the purely linear frame.

II. SOME IMPORTANT PHENOMENA IN ROTOR DYNAMICS

We will now discuss some of the important aspects of rotor dynamics. We will see more particularly the notions of critical velocities, instabilities related to the rotating damping and the role that the dissymmetries can play on the dynamics of the rotors.

A-Critical speeds

The critical speed corresponds to the speed where the unbalance excitation coincides with one of the natural frequencies of the system. For the machines made up of organs with important moments of polar inertia, one notes a strong dependence of the eigen modes vis-à-vis the speed of rotation due to the gyroscopic effects. Thus, we observe the duplication of the eigen modes of the system (for the case of an axisymmetric system) due to the gyroscopic forces as follows:
- A direct precession (FW) where the rotor rotates in the same direction as its precession. Then, under the gyroscopic effects, the associated resonant frequency increases.
- Retrograde precession (BW), in which the rotor rotates in the opposite direction of its precession movement, which gives rise to a softening effect and therefore a fall in the critical speed.

B- Instability due to rotating damping

Depreciation corresponds to one of the determining factors for sizing systems and more particularly for studying the stability of rotating machines. Indeed, the damping (particularly that of the rotating parts) can be responsible for unstable phenomena at high speed, which can lead to the rupture of elements composing the rotor. It is essential to be able to estimate the damping proportions brought on both the fixed parts and the rotating parts, in order to guarantee the integrity of the system.

C-Dissymmetries

Commonly the rotors are designed as axisymmetric. Nevertheless, the stator may have functional characteristics that invalidate this assumption. In this case, the dynamics of the machine will present some differences with respect to the axisymmetric case. The dual modes give way to two simple modes of distinct frequencies leading, as in the case of axisymmetry, to a direct mode and a retrograde mode (figure .1).(Lalanne and Ferraris)[21] .In this case, the retrograde modes are solicited

by the synchronous excitation and the number of critical speeds is multiplied by 2, compared to the axisymmetric case.

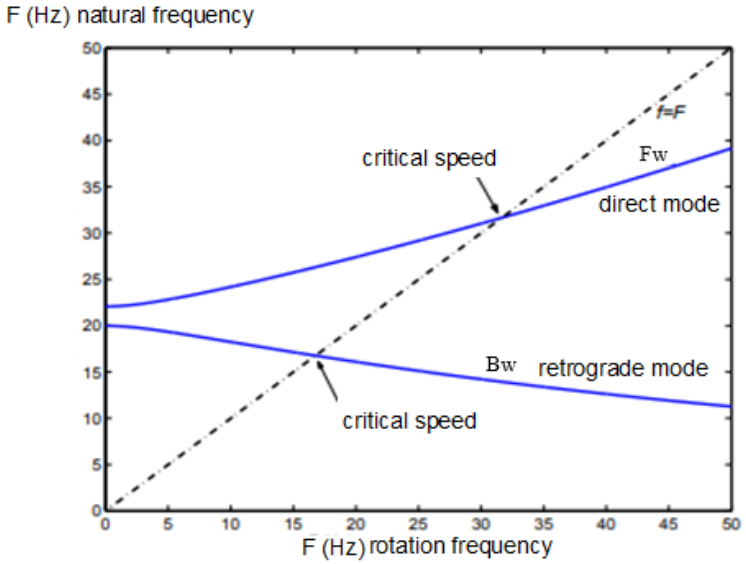

Figure 1.Exemple d'un diagramme de Campbell pour un rotor avec des supports orthotropes.

D- The modal orbit

The points situated in the rotor generator axis describe by the rotor rotation motion and due to the eigenmode of the orbits which have shapes according to the phenomenon to which [22] is envisaged (circular for a symmetrical rotor damped, elliptical name for a rotor asymmetric name depreciated ....) These orbits are generated according to two possible precessions :

- A direct precession where the orbits are described in the same direction as the rotor rotation speed Ω, in which case under the gyroscopic effects, the associated resonant frequency increases.
- A retrograde precession (inverse), where the orbits are described in the opposite direction as the direction of the rotational speed of rotor, from which a relaxation effect and thus a fall of the critical speed.

E-Stability analysis

The stability analysis in the study of vibratory and dynamic behavior of a flexible rotor is necessary since it considered a dynamic system governed by systems of differential equation. The definition of stability covers the definition of Laypunov for equilibrium stability analysis and Poincaré's definition for the concept of orbital stability [23].

We can predict the thresholds of the instability of a dynamic system and in particular in rotor dynamics from the various techniques:

- Sign of the real part of the complex eigenvalues of the equation system in free motion. If the eigenfrequency is given by s = -a ± jb, the only instability is determined when a becomes negative (real positive part), With this criterion one can estimate the frequency as well as the mode for which the system will become unstable.

The Routh-Hrwitz criterion makes it possible to analyze the stability of autonomous systems [24]. The use of this criterion is interesting for systems with a low number of degrees of freedom, for which analytical expressions of the characteristic polynomial associated with the disturbed movement can

be deduced. It becomes, however, complex for systems with a large number of degrees of freedom. In addition, this criterion does not provide the frequency of instability.

III. EQUATIONS OF MOTION

By integrating the kinetic energies and the strain energies into the Lagrange equations, we obtain :

$$\frac{d}{dt}\left(\frac{\partial T}{\partial \dot{q}_1}\right)-\frac{\partial T}{\partial q_1}+\frac{\partial U}{\partial q_1}=Fq_1$$

(1)

$$\frac{d}{dt}\left(\frac{\partial T}{\partial \dot{q}_2}\right)-\frac{\partial T}{\partial q_2}+\frac{\partial U}{\partial q_2}=Fq_2$$

(2) The equations of motion ; in matrix form, write:

$$M\ddot{x}+C(\Omega)\dot{x}+Kx=F(t) \quad (3)$$

M, C and K are the mass matrices, the gyroscopic effect and stiffness, respectively.F: unbalance, bearing, asynchronous force, or other.

$$x=[q_1,q_2]^{'} \quad (4)$$

A- Own frequencies of the rotor

The eigenvalues of the rotor as a function of the speed of rotation are given by:

$$m\ddot{q}_1-a\Omega\dot{q}_2+K_1q_1=0 \quad (5)$$

$$m\ddot{q}_2-a\Omega\dot{q}_1+K_2q_2=0 \quad (6)$$

Or : « a » represents the gyroscopic effect

m : the mass

k1, k2 : stiffness

When stopped (= 0)

$$\omega_{10}=\sqrt{\frac{K_1}{m}} \quad (7)$$

$$\omega_{20}=\sqrt{\frac{K_2}{m}} \quad (8)$$

Turning (≠ 0)

The expressions of the eigenvalues are given according to the speed of rotation in the form:

$$\omega_1=\left[\frac{\omega^2_{10}}{2}+\frac{\omega^2_{20}}{2}+\frac{a^2\Omega^2}{2m^2}-\sqrt{\left(\frac{\omega^2_{10}}{2}+\frac{\omega^2_{20}}{2}+\frac{a^2\Omega^2}{2m^2}\right)^2-\omega^2_{10}\omega^2_{20}}\right]^{1/2} \quad (8)$$

$$\omega_2=\left[\frac{\omega^2_{10}}{2}+\frac{\omega^2_{20}}{2}+\frac{a^2\Omega^2}{2m^2}-\sqrt{\left(\frac{\omega^2_{10}}{2}+\frac{\omega^2_{20}}{2}+\frac{a^2\Omega^2}{2m^2}\right)^2-\omega^2_{10}\omega^2_{20}}\right]^{1/2} \quad (9)$$

IV. METHODOLOGY

The main objective of this work is the study the Campbell scheme, which represents the evolution of self-repetition as a function of spin velocity and the calculation of unbalance responses mainly during the passage of critical velocity. In using the finite element method.We designed a mathematical model under the name of Nelson rotor in a matlab program containing the engineering data of the Nelson rotor element (tree data, disk data, The geometric data of the element carrying the Nelson rotor .In addition to the matrices of stiffness and damping in the form of a set of nodes and elements to calculate the existing stiffness and frequency values in the presence of the speed of 4800-28800 rpm .This calculation mode must be able to give the geometry of the rotor in finite elements. The search for eigenvalues is a fundamental operation in the study of rotor dynamic.

A- Model

The model considered is a Nelson rotor [25]. Fig. 2, which is a 0.355 (m) long overhanging steel shaft of 14 different cross sections. The shaft carries a rotor of mass 1.401(kg) and eccentricity 0.635(cm) at 0.0889(m) from left end and is supported by firstly two bearings at a distance of 0.1651(m) and 0.287(m) from the left end respectively. Six stations are considered during harmonic analysis as shown in Fig.1, where station numbers denote different nodes in themodel (1) Left extreme of shaft, (2) Disc, (3) First bearing node, (5) Between the two bearings, (4) Second bearing node and (6) Right extreme of shaft. A density of 7806 kg/m3 and elastic modulus 2.078E11 n/m2 were used for the distributed rotor and a concentrated disk with a mass of 1.401 kg,polar inertia 0.002 kg.m2 and diametral inertia 0.00136 kg.m was located at station five.

The following cases of bearings were analyzed :

a) Symmetric orthotropic bearings

b) Fluid film bearings.

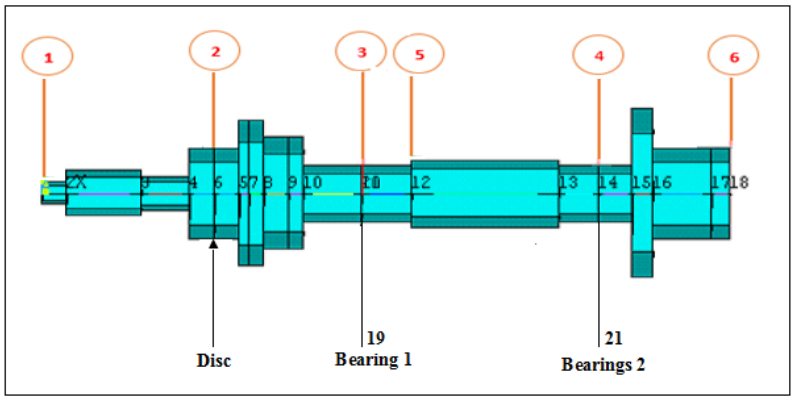

Figure 2. Model of Nelson rotor with various sections, disc and bearings Numbers indicate station numbers

B- Calculation of the Eigen values of a system

We designed a mathematical model under the name Nelson rotor in a Matlab software that contains the engineering data of the Nelson rotor element (shaft data, disk data, bearing data). In addition to the Matrices of the stiffness and damping in the form of a set of nodes and elements to calculate the values of the existing stiffness and frequency in the presence of the speed 4800-28800 rpm. Table 1.

Element Node No	Node Location (cm)	Bearing and Disk	Inner Diameter (cm)	Outer Diameter (cm)
1	0.0		0.0	0.51
2	1.27		0.0	1.02
3	5.08		0.0	0.76
4	7.62		0.0	2.03
5	8.98	Disk	0.0	2.03
6	10.16		0.0	3.30
7	10.67		1.52	3.30
8	11.43		1.78	2.54
9	12.70		0.0	2.54
10	13.46		0.0	1.27
11	16.51	Bearing	0.0	1.27
12	19.05		0.0	1.52
13	22.86		0.0	1.52
14	26.67		0.0	1.27
15	28.70	Bearing	0.0	1.27
16	30.48		0.0	3.81
17	31.50		0.0	2.03
18	34.54		1.52	2.03

C. Resolution algorithm

The algorithm for calculating the eigenvalues of a homogeneous system is described in Figure .3. calculations are done with the Matlab programming code.

• Algorithm for calculating the eigenvalues of a system

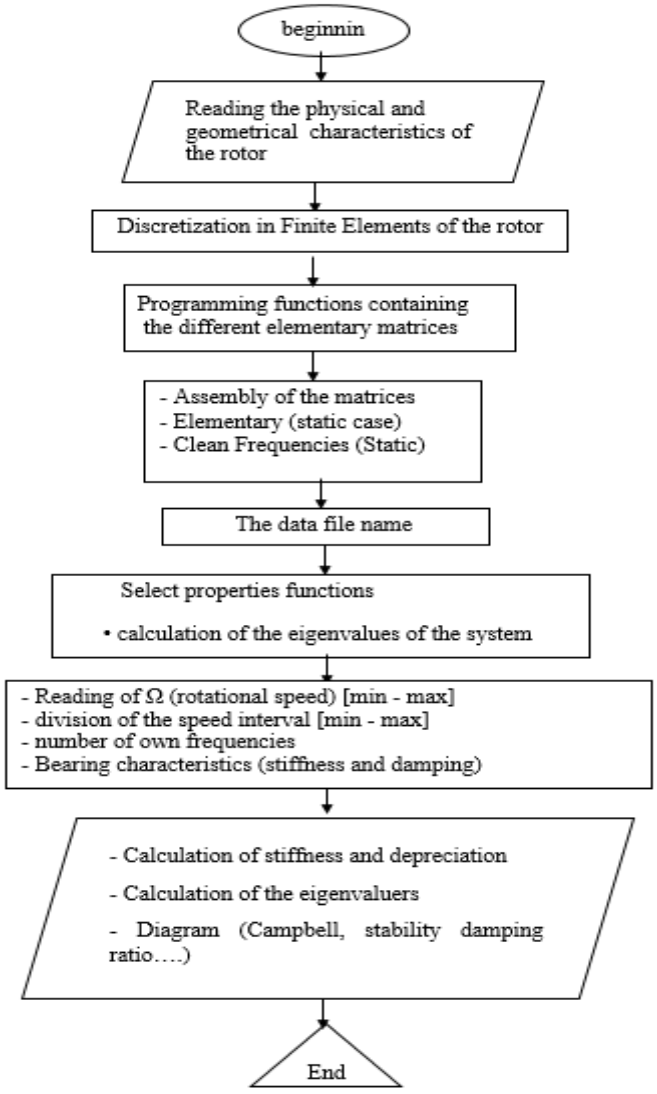

Figure .3. Algorithm for calculating the eigenvalues.

V. RESULTS AND DISCUSSION

A-Data of fluid film bearings

The shaft is supported by two fluid film bearings whose stiffnesscoefficient Table .2 was calculated by Matlab as follows :

Dynamic Coefficients of Hydrodynamic Bearings			
Stiffness coefficients (N/m)			
K_{yy}	K_{yz}	K_{zy}	K_{zz}
7.7539E + 007	2.3381E + 008	-5.4601E + 008	1.3399E + 008
1.3594E +008	5.8365E + 008	-8.412E + 007	1.4718E + 008

Table .2: Dynamic coefficients of hydrodynamic bearings.
Stiffness coefficients (N / m).

While the damping components are = = 1752 (Ns / m). The imbalance response for an eccentricity of the disk center of 0.635 (cm) at the second station was determined for a range of speeds from 4800 to 2800 rpm.

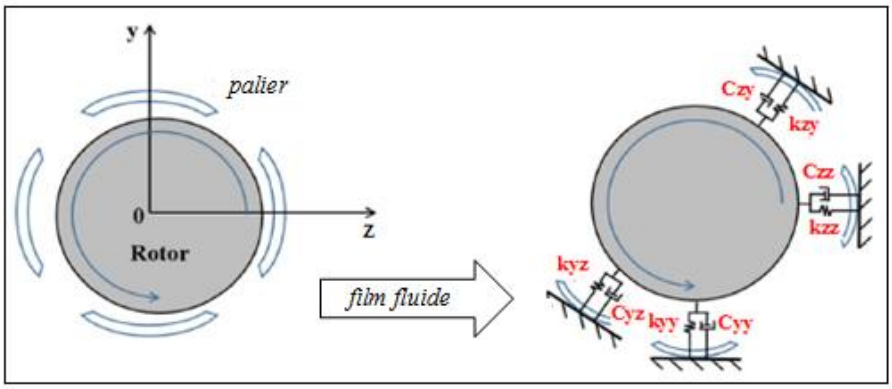

Figure .4. Schematic view of the rotor on the bearing supports and idealization of the fluid film coefficients

The Matlab program also provided us with a model for Nelson rotor with various sections, disc and bearings.Fig.5.

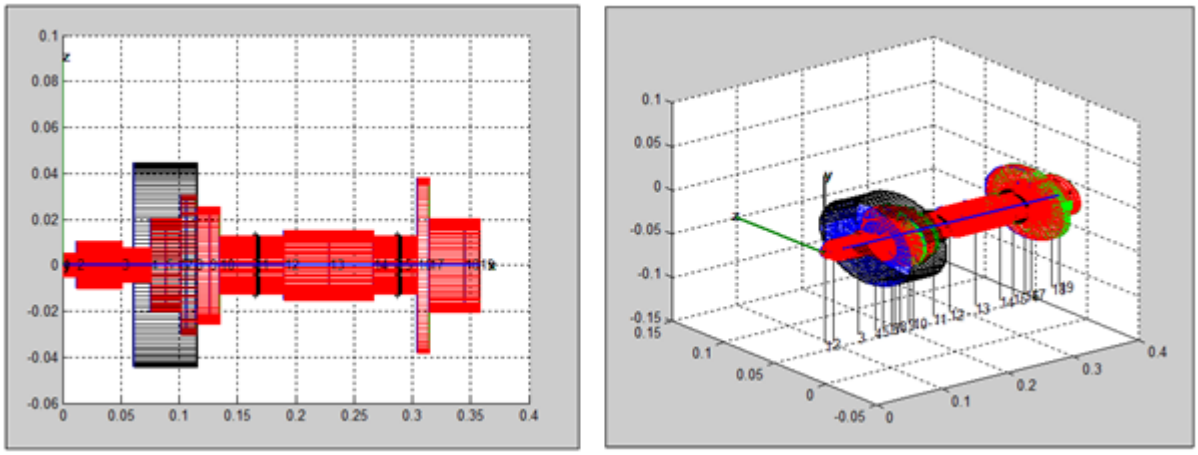

Figure 5. Nelson rotor with various sections.

B- Estimated critical speeds

1-The Campbell Diagram

Figure 6 Shows the Campbell diagram of the rotor-shaft system, when the shafts internal material damping is considered. The graph is plotted by using the whirl frequencies (obtained from the imaginary part of the eigenvalues), and there are two positions, the first position in reverse rotation "BW", where the rotor rotates in the opposite direction. The second position is the rotation "FW", where the rotor rotates in the direction of rotation. The critical speed corresponding to the first position and the critical speed corresponding to the second position appear in Table.3.

Table.3 lists the values of the first critical speeds identified :

Mode	Critical speed (Hz)	Critical speed (rpm)
5	3.3837e+002	2.0302e+004
6	4.0607e+002	2.4364e+004

Table .3. Critical speeds

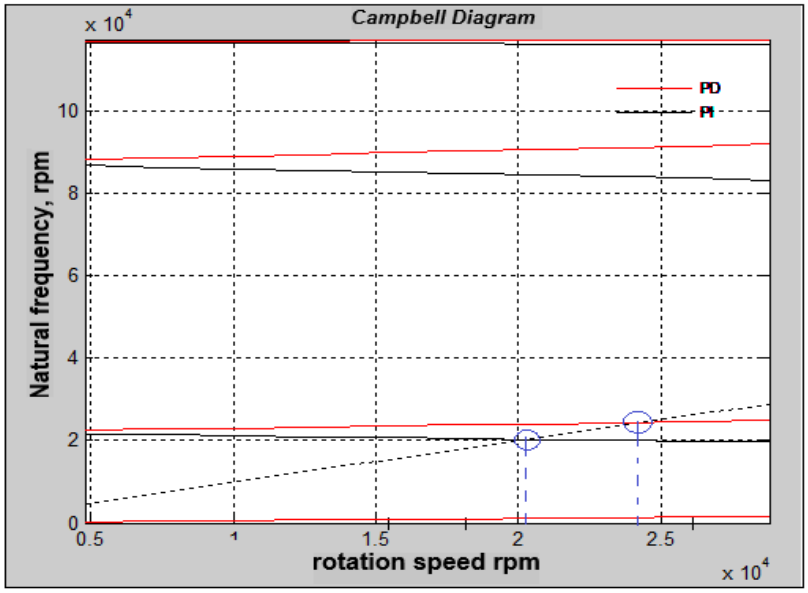

Figure 6. Campbell Diagram.

Results for the Stability Chart, Damping Report Diagram, Mode Shapes, Elliptical Orbits, Mode Shape Precession, Root Locus Diagram. Are presented by matlab program as follows.

2. Stability diagram

The stability diagram (Figure .7) presents the evolution of the damping constant as a function of the rotational speed. We observe through the diagram that the values of the damping coefficient are negative and indicates that the rotor is stable.

Onset of instability speeds

Mode	(Hz)	(rpm)
1	0.0000e+000	0.0000e+000
2	0.0000e+000	0.0000e+000
3	0.0000e+000	0.0000e+000
4	0.0000e+000	0.0000e+000
5	0.0000e+000	0.0000e+000
6	0.0000e+000	0.0000e+000
7	0.0000e+000	0.0000e+000
8	0.0000e+000	0.0000e+000
9	0.0000e+000	0.0000e+000
10	0.0000e+000	0.0000e+000

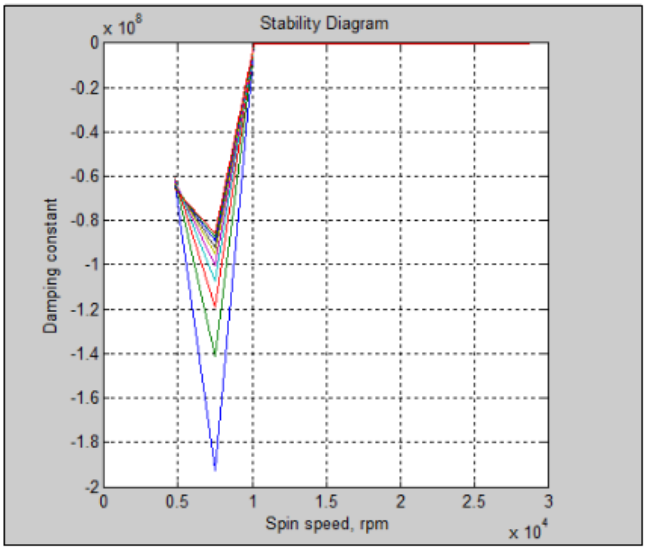

Figure .7. Stability diagram

3. damping ratio

The damping ratio diagram. Figure .8, show the evolution of the damping ratio as a function of the speed of rotation, we note that the system regardless of the speed of rotation (4800-28800tr / min), rotor system operation always stable.

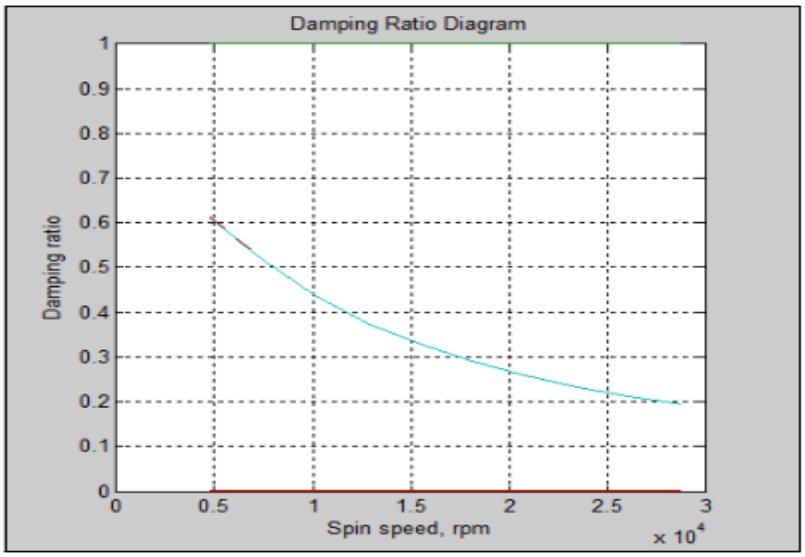

Figure 8. damping ratio diagram.

4. Mode Forms and Mode Form Precession

Table.4 gives the result of the shapes of the modes and the shape precession and the rotational speed for the modes. We observe that the modes 1, 2,3, 4, 6, 8, 10 are direct precession (the rotor rotates in the direction of rotation), and the modes 5, 7,9, are inverse precession (the rotor rotates in the opposite direction).

Modes	Precession	Spin speed rpm
1	direct	FW=0
2	direct	FW=0
3	direct	FW=281.8067 rpm
4	direct	FW=281.8176 rpm
5	inverse	BM=21645.764 rpm
6	direct	FW=22513.8662 rpm
7	inverse	BM=86691.2517 rpm
8	direct	FW=88125.162 rpm
9	inverse	BM=116503.6699 rpm
10	direct	FW=116711.5916 rpm

Table.4. Forms of Modes and Precession of Formsat 4800 rpm.

Figure .9 gives relative deviation as a function of tree length and confirms the results obtained in Table 4.

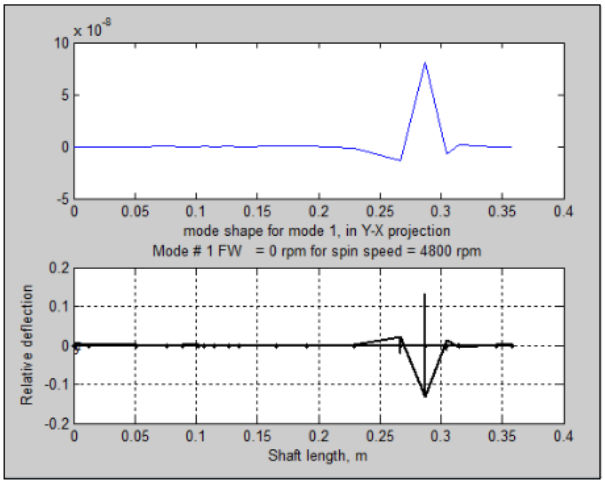

Mode 1

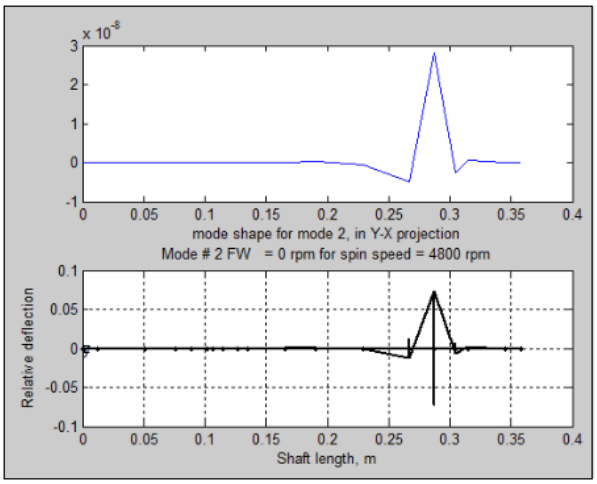

Mode 2

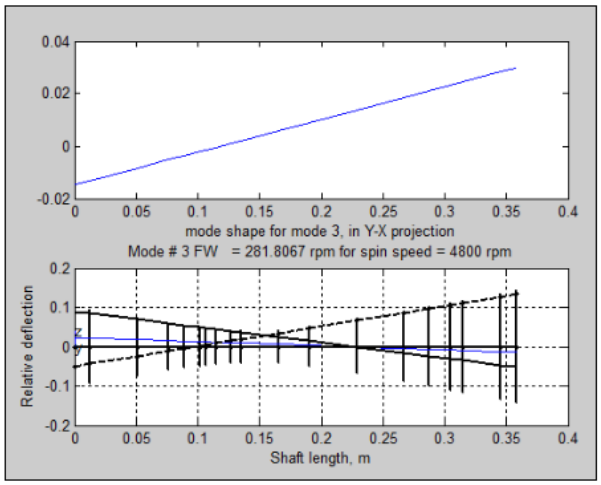

Mode 3

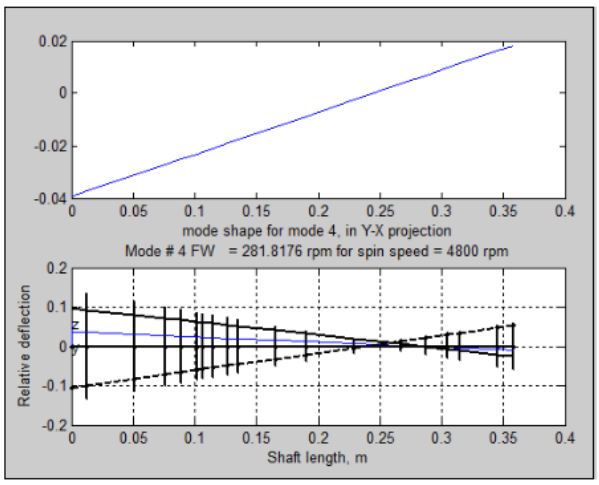

Mode 4

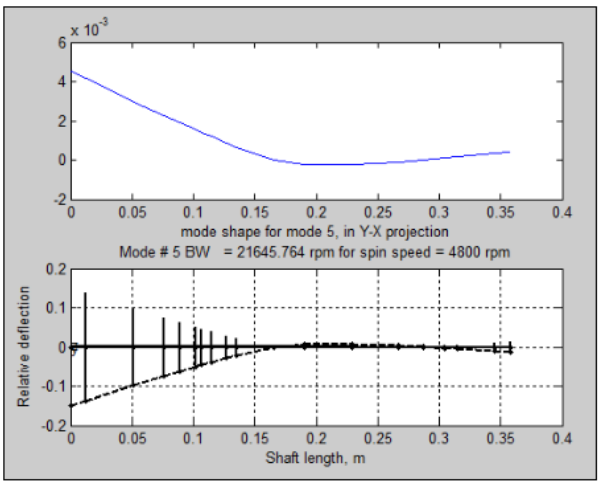

Mode 5

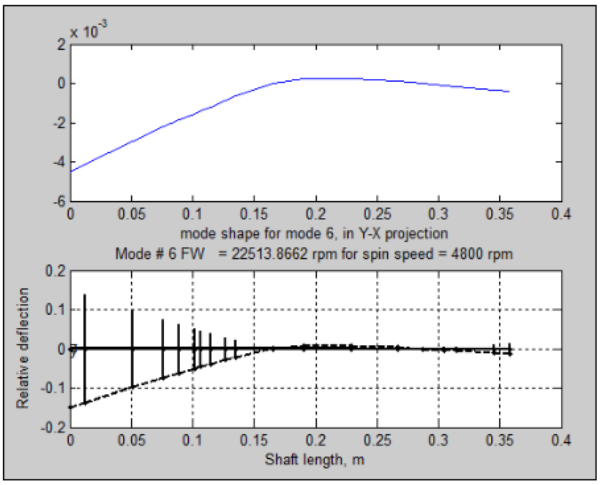

Mode 6

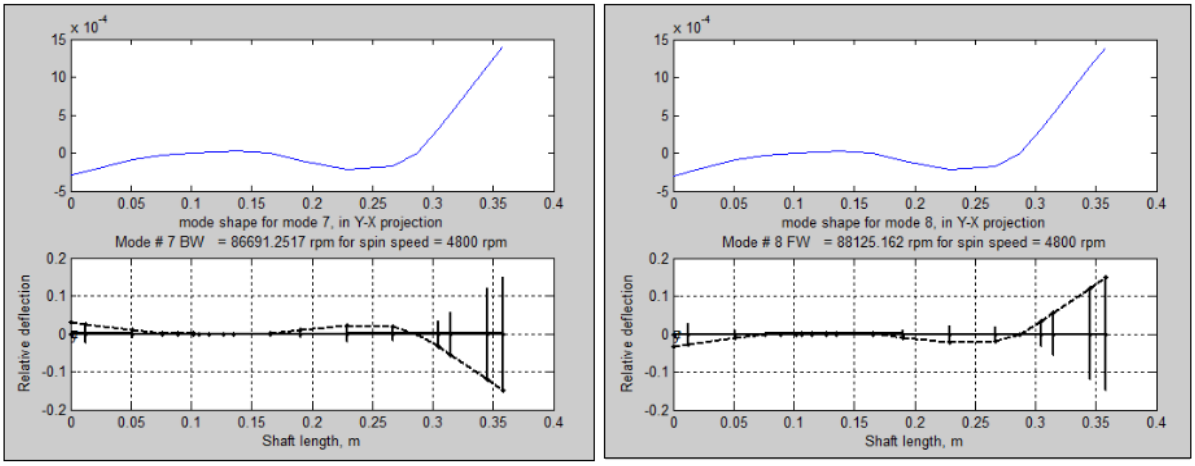

Mode 7 Mode 8

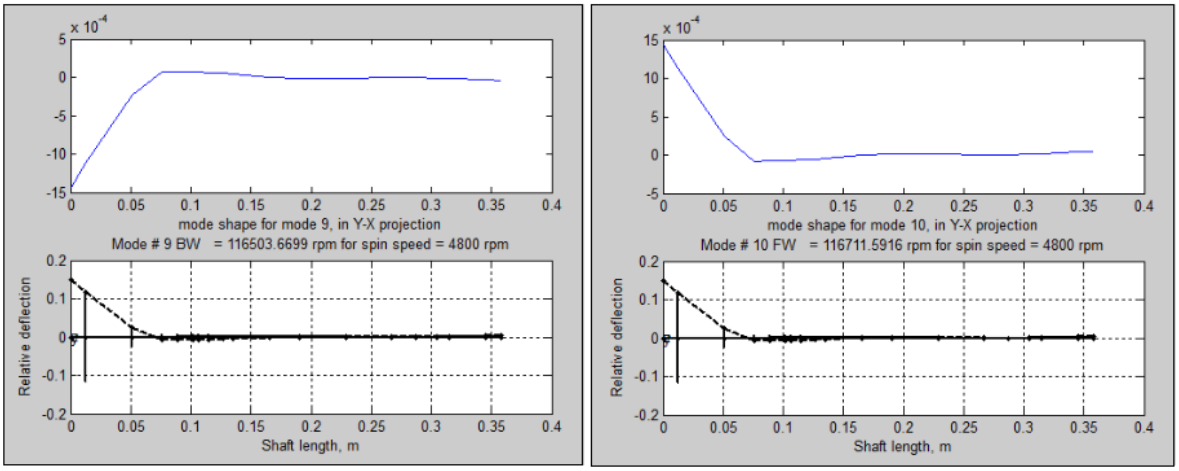

Mode 9 Mode 10

Figure .9. Forms of Modes and Precession of Forms of Modes

at 4800 rpm.

4. Elliptical Orbits

We see the representation of the orbits on the measurement planes, For the rotation speed 4800 rpm, the orbits have forme :

Circular for a symmetrical rotor damped, elliptical name for a rotor asymmetric shape.

The direction of precession of the orbits obtained is represented graphically in Figure .10 with the beginning of the orbit represented by a circle and the end represented by a star. The figure shows that the orbits C1, C2, C6, C10 are described in the same sense as the rotational speed of the rotor Ω, in which case under the gyroscopic effects, the associated resonance frequency increases.

And the C5 orbits are described in the opposite direction as the direction of the rotational speed of rotor, from which generated a softening effect and therefore a fall of the critical speed.

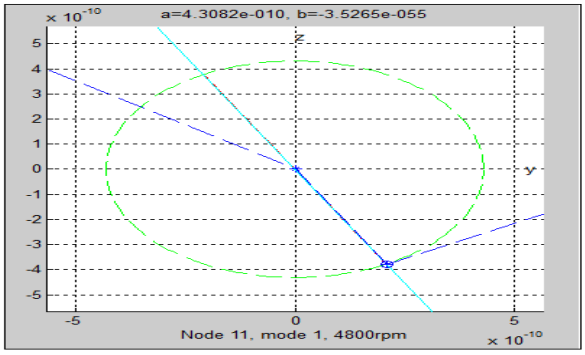

C 1

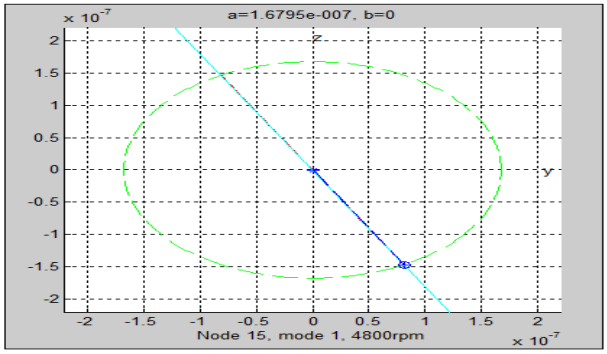

C 2

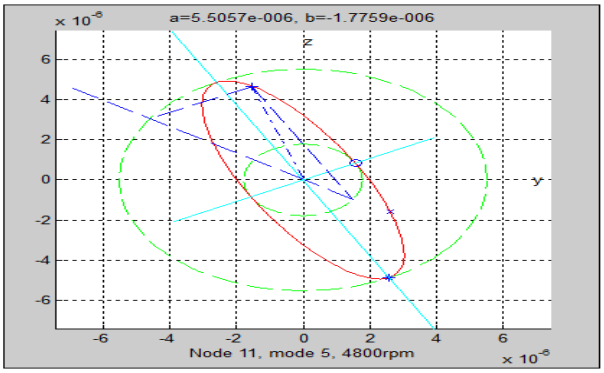

C 5

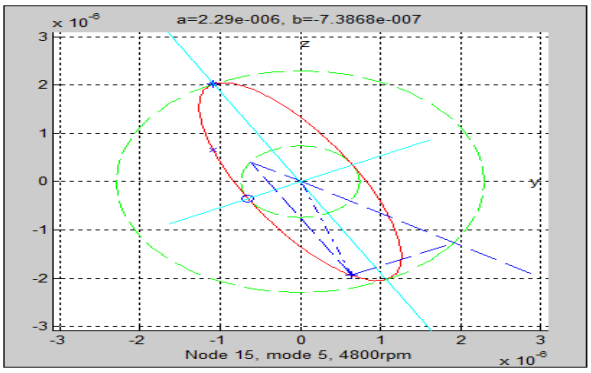

C 5

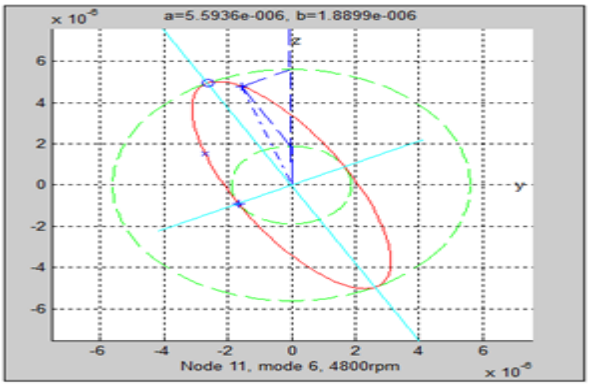

C 6

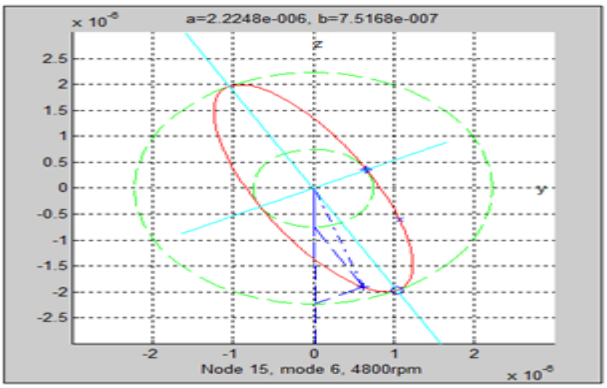

C 6

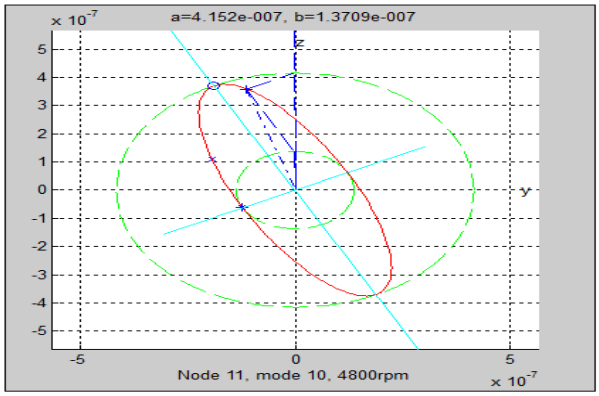

C 10

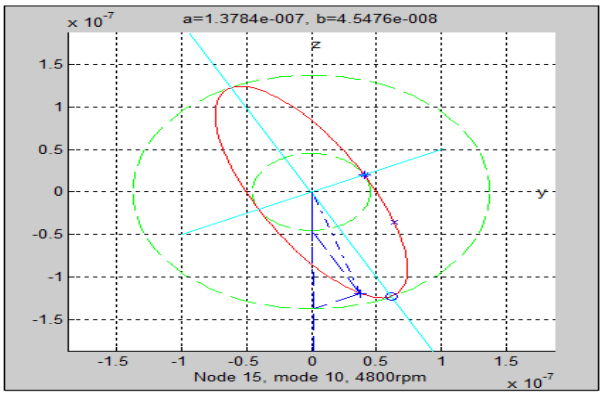

C 10

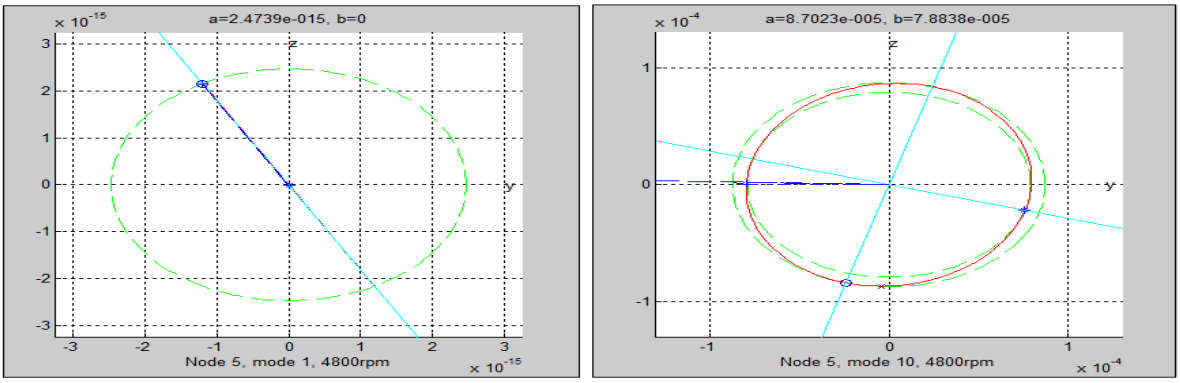

C1 C10

Figure 10. Orbits at 4800 rpm

5. root locus diagram

The root locus diagram figure 11. Shows the evolution of the damping constant as a function of the natural frequency. For example, we notice the direction of the modes, 5, 7, 9 from left to right (odd), so the mode a reverse precession. And the direction of the modes 4,6, 8,10 from right to left (even), so the direct precession mode.

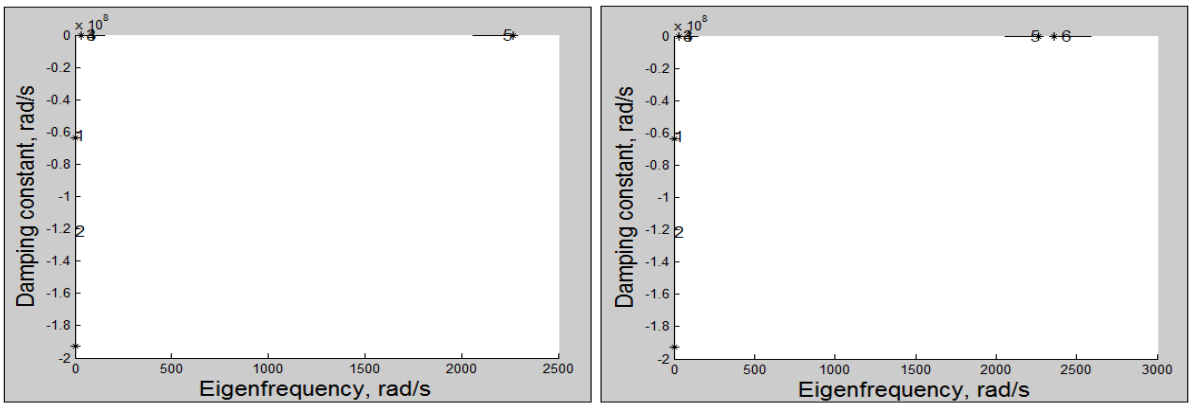

Mode 1 / mode 5 **mode 1 / mode 6**

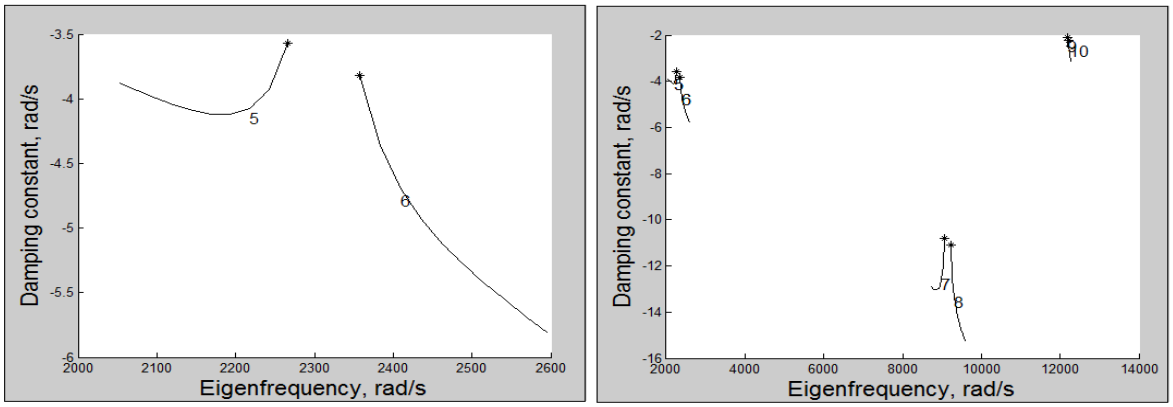

Mode 5 / mode 6 **mode 5/ mode 10**

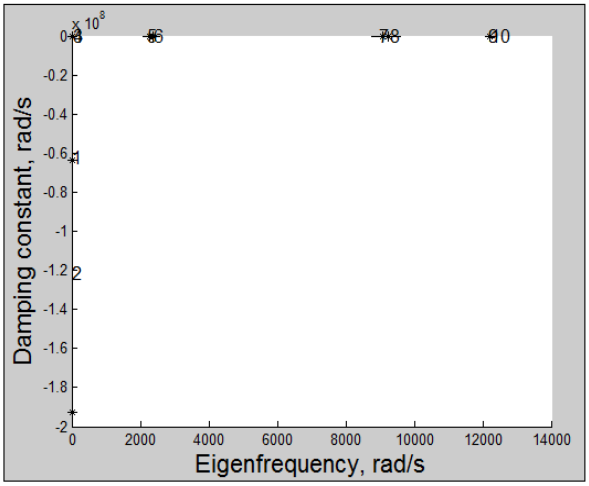

Mode 1/mode 10

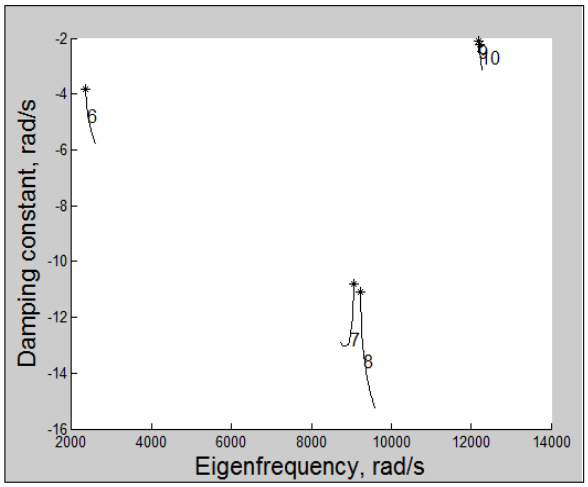

mode 6/mode10

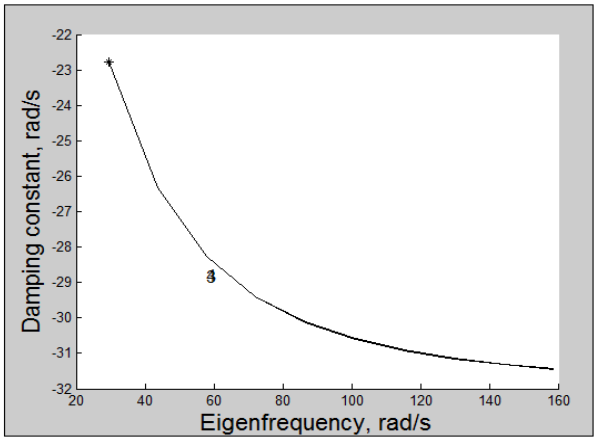

Mode 3/mode 4

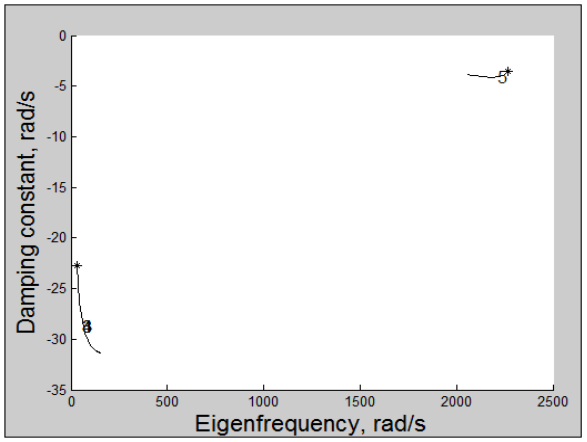

mode 3 /mode 5

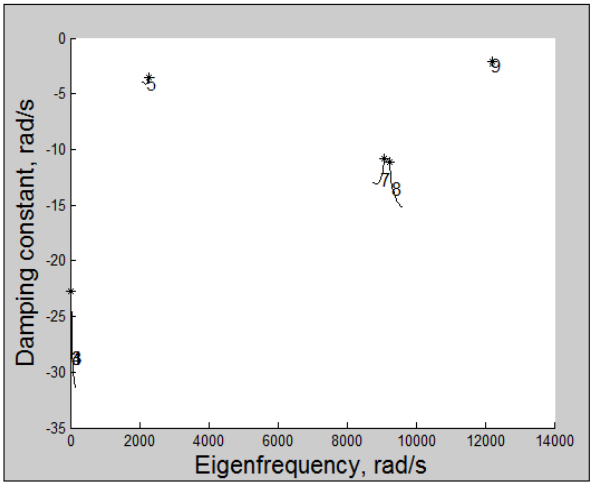

mode 7/mode 9

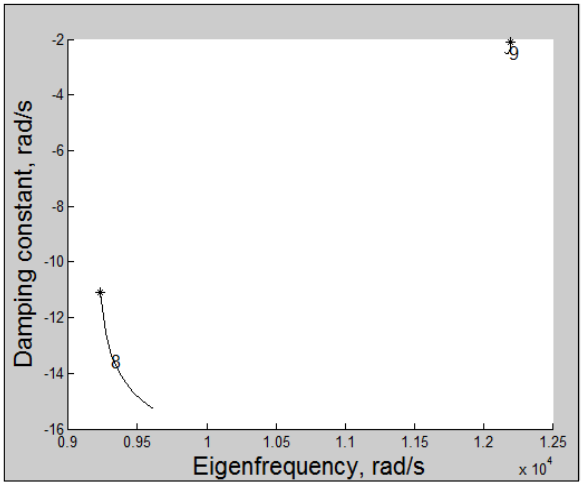

mode 8 /mode 9

Figure .11. Root Locus Diagram

VI. Conclusions

The general equations of a uniformly rotated rotor have been developed in this work using the finite element method. It is more adapted to model the real systems insofar as one knows the dynamic characteristics of the bearings for example. It allows the study of all modes of vibration of the rotor. It is also modular because each element of the rotor has its own characteristics.The effects of rotary inertia, and internal damping were included in the analysis. Study also obtained the variation of amplitude response with frequency as it is important for minimizing the noise of the rotor. The increasing amplitude increases the noise of the rotor. This analysis gives the alternate procedure of finding the critical speed that is harmonic analysis.

References

[1.] G. Genta. Vibration of Structures and Machines : Practical Aspects. Springer-Verlag, 1999.

[2.] D. Childs. Turbomachinery Rotordynamics : Phenomena, Modeling, and Analysis. Wiley- Interscience, 1993.

[3.] A. Muszynska. Forward and backward precession of a vertical anisotropically supported rotor. Journal of Sound and Vibration, 192(1) :207.222, 1996.

[4.] M. Dias-Jr, S. J. Idehara, A. L. A. Mesquita, and U. A. Miranda. On the simultaneous forward and backward whirling of flexible rotors : Numerical analysis and experimental veri_cation, 30/09/2002, sydney, australia. In IFToMM - Sixth International Conference on Rotor Dynamics, Sydney, Australia, 2002.

[5.] C. Rao, R. B. Bhat, and G. D. Xistris. Simultaneous forward and backward whirling in a jeffcott rotor supported on dissimilar hydrodynamic bearings. Journal of Sound and Vibration, 203(4) :707.716, 1996.

[6.] C. Rao, R. B. Bhat, and G. D. Xistris. Experimental verification of simultaneous forward and backward whirling at different points of a jeffcott rotor supported on identical journal bearings. Journal of Sound and Vibration, 198(3) :379.388, 1996.

[7.] M. Sakata, M. Endo, K. Kishimoto, and N. Hayashi. Secondary critical speed of flexible rotors with inertia slots. Journal of Sound and Vibration, 87(1) :61.70, 1983.

[8.] Y. Kang, Y. P. Shih, and A. C. Lee. Investigation on the steady-state responses of asymmetric rotors. ASME Journal of Vibration and Acoustics, 114 :194.208, 1992.

[9.] E. Hashish and T. C. Sankar. Finite element and modal analyses of rotor-bearing systems under stochastic loading conditions. ASME Journal of Vibration, Acoustics, Stress, and Reliability in Design, 106(1) :80.89, 1984.

[10.] Hamdi Taplak, Mehmet Parlak, (2012) "Evaluation of gas turbine rotor dynamic analysis using the finite element method," Measurement 45 1089–1097.

[11.] B. Gurudatt, S. Seetharamu, P. S. Sampathkumaran and Vikram Krishna, (2010) "Implementation, of Ansys Parametric Design Language for the Determination of Critical Speeds of a Fluid Film Bearing Supported Multi Sectioned Rotor with Residual Unbalance Through Modal and Out Of Balance Response Analysis," Proceedings of the World Congress on Engineering Vol II.

[12.] R. Sinou, T.N. Baranger, E. Chatelet, G. Jacquet, (2008) "Dynamic analysis of a rotating composite shaft," Composites Science and Technology 68 (2) pp.337–345.

[13.] M. Chouksey, J.K. Dutt, S.V. Modak, (2012) "Modal analysis of rotor-shaft system under the influence of rotor-shaft material damping and fluid film forces," Mechanism and Machine Theory 48, pp.81–93.

[14.] R. Whalley, A. Abdul-Ameer, (2009) "Contoured shaft and rotor dynamics," Mechanism and Machine Theory 44 (4) pp.772–783.

[15.] R. Gasch, (2008) "Dynamic behaviour of the Laval rotor with a transversecrack," Mechanical Systems and Signal Processing 22 (4), pp.790–804.

[16.] A.S. Das, M.C. Nighil, J.K. Dutt, H. Irretier, (2008) "Vibration control and stability analysis of rotor-shaft system with electromagnetic exciters," Mechanism and Machine Theory 43 (10) 1295–1316.

[17.] C. Villa, J.J. Sinou, F. Thouverez, (2008) "Stability and vibration analysis of a complex flexible rotor bearing system," Communications in Nonlinear Science and Numerical Simulation 13 (4) 804–821.

[18.] S. Lei, A. Palazzolo, (2008) "Control of flexible rotor systems with active magnetic bearings," Journal of Sound and Vibration 314 (1–2), pp.19–38.

[19.] Breńkacz Ł, Eng. Grzegorz Ż, Marta Drosińska K. (2017). the experimental identification of the dynamic coefficients of two hydrodynamic journal bearings operating at constant rotational speed and under nonlinear conditions. Polish Maritime Research 4(96) : 108-115. https://doi.org/10.1515/pomr-2017-0142

[20.] Fulaj D, Jegadeesan K, Shravankumar C. (2018). Analysis of a rotor supported in bearing with gyroscopic effects. IOP Conf. Series : Materials Science and Engineering 402(2018) : 012059. https://doi.org/10.1088/1757-899X/402/1/012059

[21.] M. Lalanne and Ferraris G. Rotordynamics Prediction in Engineering. John Wilet and Sons, 1990.

[22.] M Lanane and G.Ferraris « rotordynamique prediction in engineering » John Wiley Sons 1990

[23.] D.P.Atherton « Nonlinear Control Engineering » Van Nostrand Reinhold Company ,1975

[24.] L Meirovitch « elements of vibration analysis » Mac Graw Hill international editions, 1986

[25.] Nelson HD. (1976). The dynamics of rotor bearing system using finite elements. ASME Journal of Engineering for Industry 98(2) : 593-60. https://doi.org/10.1115/1.3438942

NOMENCLATURE

Kyy, Kyz, Kzy, Kzz	stiffness coefficients.
Cyy, Cyz, Czy, Czz	damping coefficients.
a	gyroscopic effect
k1, k2	stiffness
ω	The speed of rotation of the shaft (rd / s)
Ω	angular velocity of the shaft (rd / s)

International Journal of Innovation Engineering and Science Research
(ISSN: 2581-4591)
www.ijiesr.com

To the question of a process optimization of cast in a metal mould of automotive pistons made of grey cast iron and silumin

Denis Chemezov, Irina Medvedeva, Alexandra Strunina, Tatyana Komarova, Ivan Mochalov, Polina Nikitina
Vladimir Industrial College
Vladimir, Russian Federation

ABSTRACT

A calculation of an optimal geometry of a gating system for cast in a metal mould of automotive pistons made of grey cast iron and silumin was performed. A conclusion about surface cast defects was given by the obtained three-dimensional models of the pistons castings. It is noted that the casting made of A356 silumin is cooled (is crystallized) uniformly throughout the volume, compared with the casting made of EN-GJL-300 grey cast iron.

Keywords *– a piston, cast, a metal mould, a gating system, silumin, grey cast iron.*

I. INTRODUCTION

A piston is one of responsible parts of an internal combustion engine of a car. The piston works under severe conditions and is subjected to variable loads of various kinds. For increasing of an operation period of the piston, it is necessary to reduce errors at manufacturing of the part, defects at manufacturing of a work piece and to increase durability of the finished part by hardening of working surfaces. Cast, and in particular cast in a metal mould, is one of manufacturing methods of the work piece of the automotive piston.

This method of cast is described in the works [1 – 10]. Metal melt cools rapidly and the remote mould cavities remain unfilled in a process of cast in the metal mould. Additional melt feeding allows to avoid premature crystallization of melt in the metal mould. Required melt feeding is determined after a calculation of optimal dimensions and the elements shape of a gating system of the metal mould. A computer simulation will provide a visual view of predicted incomplete fillings in castings at a designing stage of the technological process of cast in the metal mould of the automotive pistons.

II. MATERIAL AND METHOD

The process of gravity cast of the automotive pistons in the metal mould was implemented by the method of finite element modeling in the LVMFlow software environment.

The three-dimensional solid models of the pistons castings and the gating systems were built for the calculation. The grooves for the rings and the pin bore were provided in the castings models of the automotive pistons. The model of the gating system consisted of the pouring basin (for receiving of melt jet), the vertical downsprue (for melt supply in other elements of the gating system), the gas vent (for gases withdraw from the mould cavity and control of filling it by melt) and the slit gate (for melt supply in the mould cavity).

The castings of the automotive pistons were made of EN-GJL-300 grey cast iron and A356 silumin. Initial temperatures of melts of grey cast iron and silumin were 1290 °C (the liquidus temperature is 1196.791 °C) and 710 °C (the liquidus temperature is 617.848 °C), respectively. Alloys of grey cast iron and silumin have the same CLF down in liquid state. Melt of grey cast iron has the higher CLF up than melt of silumin. Initial grains growth rates in melts at cooling were changed from 5 to 200 times. The metal mould model was made of grey cast iron and was adopted by a perfectly rigid body.

Heating of the metal mould to the temperature of 200 °C for 5 s was provided at the calculation. The process calculation of cast in the metal mould was performed by the quasi-equilibrium model taking into account convection and without segregation. The friction factor of melts flow of grey cast iron and silumin in the metal mould was taken by 0.9.

III. Result and discussion

The calculated contours of thermal modulus on the three-dimensional models of the pistons castings are presented in the Fig. 1.

Color spectrum on the models characterizes cooling uniformity (crystallization) of melt in the metal mould. According to the scale located to the right of the model, crystallization of grey cast iron in the casting skirt is approximately twice as fast as in the crown. This suggests an uneven structure of the casting of the cast iron piston after cooling. Shrinkage of the casting made of EN-GJL-300 grey cast iron is not more than 1% of the entire volume. Crystallization of silumin melt in the metal mould is uniform. Almost the entire outer surface of the casting crown of the piston is subjected to shrinkage after cooling.

It is necessary to design the rational gating system for eliminating these cast defects. This will lead to uniform and complete filling of the entire volume of the metal mould cavities by melt.

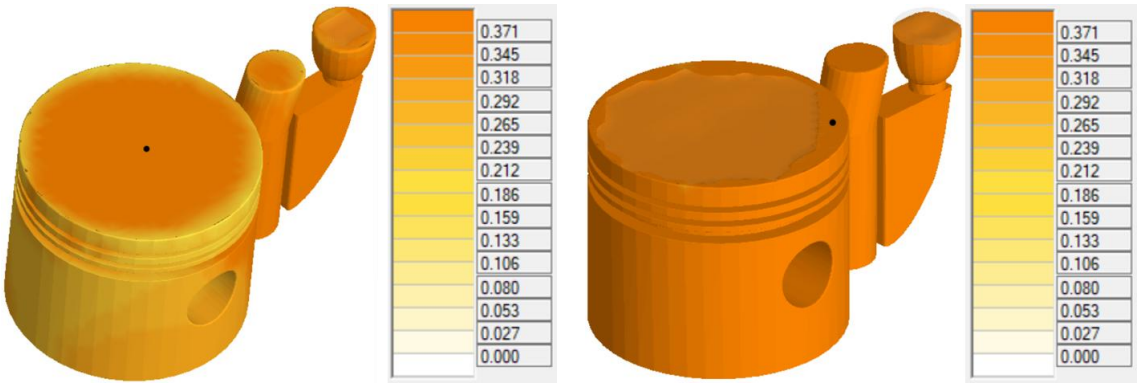

Fig. 1. The thermal modulus contours on the models of the pistons castings: *A* – EN-GJL-300 grey cast iron, *B* – A356 silumin.

The control points of the black color were set on the crowns surfaces of the castings models. A location of the control point on the crown surface of the piston casting was taken on the basis of predicted incomplete filling of the metal mould cavities by melt. Values of thermal modulus at the selected control points are the same.

The calculation results of the gating system for optimal cast in the metal mould of the cast iron and aluminium pistons are presented in the summary table I.

TABLE I. THE CALCULATION RESULTS OF THE GATING SYSTEM FOR OPTIMAL CAST IN THE METAL MOULD OF THE CAST IRON AND ALUMINIUM PISTONS.

Parameter	***Cast iron piston***	***Aluminium piston***
Alloy name	EN-GJL-300	A356
Alloy density, kg/m^3	7013.077	2425.751
Casting modulus, cm	0.522	0.544
Casting weight, kg	1.280	0.433
Pouring temperature, °C	1290.00	710.00
Minimum feed metal requirement, %	1.783	6.117
Minimum modulus ratio feeder/casting	1.200	
Feeder ratio height/diameter	1.500	
Modulus ratio neck/casting	0.800	
Feeder type	Cylinder	
Mould hardness	80.000	

Location	Top	
Minimum feeder modulus, cm	0.626	0.747
Actual modulus ratio feeder/casting	1.200	1.372
Feed metal requirement, cm^3	4.558	15.633
Feeder weight, kg	0.308	0.181
Modulus feeder neck, cm	0.418	0.435
Feeder neck dimension square, mm	16.706	17.414
Minimum feeder diameter, mm	33.412	39.829
Minimum feeder height, mm	50.118	59.743

The different volumes of melt of grey cast iron and silumin are required at the same dimensions of the pistons castings and the gating systems of the metal moulds. Melt feeding of grey cast iron in the amount of 4.558 cm^3 is required additionally for cast of the cast iron piston; melt feeding of silumin in the amount of 15.633 cm^3 is required additionally for cast of the aluminium piston. The cylindrical feeders are offered with the minimum diameters of 33.412 mm for melt supply of grey cast iron and 39.829 mm for melt supply of silumin in both cases. The ratio of the feeder height to its diameter for two designed gating systems of the metal mould was 1.5. The feeder weight in the gating system of the metal mould is reduced at cast of the aluminium piston.

IV. Conclusion

Thus, additional melt feeding of not less than 5% of the entire volume of the casting is required at cast of the aluminium pistons in the metal mould. Constancy of material properties of the piston casting is ensured by uniform cooling of silumin melt. Linear shrinkage of the casting of the aluminium piston was approximately 3.5%. Changing of the casting orientation of the piston in the metal mould (the crown is located at the bottom of the metal mould) allows to reduce linear shrinkage of material up to 0.5%. The cavities dimensions with allowance equal to the value of linear shrinkage of material must be provided at designing of the mould for cast of the aluminium pistons.

References

[1] Chemezov, D., Smirnova, L., & Bogomolova, E. (2018). Metal mold casting of cast iron and aluminium pistons. *ISJ Theoretical & Applied Science, 05 (61)*, 132-141.

[2] Chemezov, D., Osipov, T., Pesenko, A., Komarova, T., Aronova, I., & Lukyanova, T. (2018). Hardness determination of a cast iron piston after metal mold casting. *ISJ Theoretical & Applied Science, 05 (61)*, 201-203.

[3] Piątkowski, J., & Kamiński, P. (2017). Risk assessment of defect occurrences in engine piston castings by FMEA method. *Archives of foundry engineering, volume 17, issue 3*, 107-110.

[4] Wang, et al. (2011). Differential Calculation Model for Liquidus Temperature of Steel. *Steel research international, 82(3)*, 164-168.

[5] Kawasaki, S., et al. (1984). On the Secondary Cooling Control Technology for the Continuous Casting. *Direct Rolling Process Nippon Steel Technical Report, 23*, 69-76.

[6] Barozzi, P., Fontana, P., & Pragliola, P. (1986). Computer Control and Optimization of Secondary Cooling During Continuous Casting. *Iron and Steel Engineer, 63(11)*, 21-26.

[7] Lysenko, A. B., Kosynska, O. L., Gubarev, S. V., & Kravets, A. L. (2015). Thermal regimes & crystallization kinetics during casting light vitrify glass melts into a metal mold. *Machines. Technologies. Materials., Vol. 9, Issue 4*, 19-21.

[8] Rasulov, F., & Babaev, A. (2018). Surface Alloying of the Casting in the Casting Mold. *Engineering and Applied Sciences. Vol. 3, No. 3*, 64-73.

[9] Pustovalov, D. O., Labutin, V. N., Belova, S. A., & Milovanov, R. S. (2015). Determination residence time of the cast steel "Ball" in a metal mold to a temperature lined knockout. *Modern problems of science and education, №2*.

[10] Bolotina, O. & Portenko, V. A. (2018). Review of Defect Types in Metal Mold Castings. *Key Engineering Materials, Vol. 769*, 269-274.

International Journal of Innovation Engineering and Science Research
(ISSN: 2581-4591)
www.ijiesr.com

MANETs in Military Communications Design Concepts and Challenges

Dalal Alshammari
Swansea University
Bay Campus, Swansea SA1 8EN, United Kingdom

Salman Al-Shehri
Swansea University
Bay Campus, Swansea SA1 8EN, United Kingdom

ABSTRACT

The mobile tactical network (MTN) utilized for wireless military communications networks are classified as MANETS. Modern tactical communication systems are highly heterogeneous dynamic networks interconnecting many different types of users. Involving personnel, vehicles, sensors, devices and other connected equipment, the users have vastly different communication requirements while co-existing in smaller or larger geographical proximity. Unlike their commercial counterparts, MTNs pose unique characteristics with restricted bandwidth. Thus, the commercial vendors of ICT equipment do not have sufficient experience or capabilities to deliver military grade products. Rather, modification of commercial product by the original providers or third-party vendors to meet the battlefield requirements is frequently common. Comprehensive comparison of the performance and design characteristics of the commercial MANETs and their military counterparts was carried out using NS2 simulations. It was found that for scenarios requiring long-range connectivity, hierarchical routing protocols give the most accurate performance predictions for MTNs. Further, it is necessary to consider the sizes of various military units, different topology area size, warfighting platforms and combat mission types. Finally, it is argued that many commercial off-the-shelf (COTS) technologies can be adopted for their use in MTNs, even though it requires a lot of additional efforts to overcome challenges not considered by the commercial solutions.

KEYWORDS: *COTS, MTNs, METREICS*

I. INTRODUCTION

In the past few decades, several commercial MANETs research projects have been conducted. These studies have used various metrics based on either 802.11 or short-range communications standards. However, the commercial use of large-scale MANETs appears to be non-existent. One reason is much easier deployment and management of systems with the dedicated infrastructure such as in cellular networks [1].

However, in some natural disasters or military operations the wired infrastructure can be damaged or not always applicable. Therefore, tactical MANETs are used extensively by military units with emphasis on security, range and integration with existing systems. These MANETs are enhanced by self-forming multi-hop capabilities to improve their flexibility and coverage, and to cope with a number of specific challenges in geographical areas. A major goal towards the MTNs evolution is to provide accurate, valuable and timely information for many different types of users with heterogeneous communications and computing requirements such as in the current C4ISR systems [2]. The users are represented by sensors, surveillance satellites, unmanned aerial vehicles (UAVs), airborne platforms,

vehicles, and ground troops. The MTNs, however, very different from generic MANETs. For example, The MTNs are typically operated with restricted bandwidth in very high and ultra-high frequency bands (UHF and VHF) with different propagation loss properties [3]. The understanding of networks properties is important to effectively evaluate networking solution options pragmatically. On the other hand, security is a main concern in the establishment of MTNs. Mobile nodes are deployed in unsafe, unpredictable hostile environments makes the networks susceptible to a combination of possible attacks [4].

The currently available COTS technologies are major drivers of military communications needs. Recently, various military systems continue to adapt commercial technologies to military applications such as satellites, smart devices and sensors. However, the limitations to commercial COTS products adoption primarily arise due to the special requirements of soldiers at the tactical edge. The purpose of this paper is thus to investigate the differences between military and commercial applications of MANETs including the requirements for communications services, network topology, and the performance metrics. The study focuses on the deployment and operation of MTNs at the tactical edge of the battlefield theatre. A corresponding framework is created to support decisions on what technologies and solutions should be included in future generations of MTNs. The contents of the next sections are as follows. The effective adoption of commercial information and communication technologies (ICT) at the tactical edge of the battlefield is discussed in Section II. The main characteristics of MTNs such as the heterogeneity and the properties of physical radio links are investigated described in Section III and IV, respectively. The effect of protocol type and operation area size in MTNs are examined in Section V including realistic modeling of nodes mobility and radio wave propagation conditions. Conclusions are given in Section VI.

II. The Integration of COTS Radios into MTNs

The recent advances in ICT also strongly impact the design of MTNs, especially at the tactical edge. The ICT reduce the time to deployment, provide advanced abilities and reduce the operational cost of MTNs. The COST products provide new opportunities for their use in the military domain which did not exist previously [5]. We can consider at least two perspectives to compare COTS based MANETs and their military counterparts.

From the technology perspective, the COTS solutions that may be useful in tactical scenarios are cognitive radio (CR) networks, software defined (SDR) networks, and autonomous networks [6]. Many tactical networks rely extensively on existing public protocols particularly at the network and transport layers [7], and use the Internet protocol (IP) including IPV6 version for traffic backhaul [8]. The Global Information Grid (GIG) is the main infrastructure and enterprise solution for tactical communications developed by the Department of Defence (DOD). It employs a mixture of many military proprietary and public COTS technologies. However, most military users consider the use of public COTS technologies to present a severe security threat, since the 3rd parties may have accurate knowledge of the functioning and structure of some internal components and subsystems. Using the COTS security solutions in MTNs is often challenging of even undesirable [9].

From the economic perspective, the economies of scale are vital for offering affordable commercial products. This is more difficult to achieve for the military products, even though the demand for cyber security solutions, navigation systems and UAVs has increased significantly in recent years. The defence manufacturers are now focusing on advancing the lightweight electronics, small antennas, and other radio frequency (RF) technologies. The COTS hardware and software is finding its way to the Internet of Things (IoT) in the military C4ISR structures [10] . Since the level of financial support determines the achievable capabilities and performance of technology, it is likely the commercial drivers will influence the development of military networks much more in near future than ever before.

A. *Technology challenges at the tactical edge*

The conditions encountered by the MTNs are vastly different from those assumed in the deployment of commercial ICT products. Hence, the military sector has a long history of developing its bespoke technological solutions. The cost benefits of COTS solutions together with careful planning create new opportunities to use these technologies in military applications. However, the cheap solutions may entail the security and robustness concerns. One has to also consider typical radio communication trade-offs between the capacity, range and data rates. In order to serve much higher demands for data rates, the newer MTNs are primarily using the larger bandwidth between 4.4 to 5.4 GHz under more line-of-sight (LOS) conditions whereas the legacy MTNs were designed for the 1350-2690 MHz frequency band and BLOS transmissions. Overall, the challenges in using COTS solutions in military communications can be summarized as follows [11]:

1) Insufficient support of mobility to the degree encountered in MTNs.

2) Commercial pressures for short development cycles leading to frequent technology updates is undesirable in military applications.

3) The market dynamics for military products and the resulting returns on investment are very different from the commercial sector.

4) The commercial vendors of ICT equipment do not have sufficient experience or capabilities to deliver military grade products, for example, to guarantee the quality of service (QoS) over wide range of operating and often quite adverse conditions.

5) The cost efficiency of COTS solutions may be completely offset by lack of reliability and performance guarantees in realistic military environments.

B. *Unique technological requirements*

The barriers to adoption of commercial ICT in the military context primarily arise due to unique requirements at the tactical edge and involve the policy, environmental and technical considerations including, but not limited to, the robustness of service provisioning and information assurance. In addition, the MTNs have significantly stringent security requirements than the commercial MANETs. Therefore, a direct adoption of COTS technologies without adjustment is not recommended [12]. In some applications, the constraints of the original COTS design can be accepted, for example, the commercial-grade radios can operate successfully provided that the mobility of nodes in MTNs is limited even though the full spectrum management may be problematic [13]. It is useful to recognize that the latest function-rich COTS technologies may be less suitable for use in military systems, and that their adoption may still requires significant purpose-driven research and further development [14].

III. Exploitation of MTNs Heterogeneity

The overall goal for research on heterogeneous networks is "To enable defense users to reliably obtain and share necessary and timely information in the right form over an integrated heterogeneous dynamic network which is scalable and evolvable" [15]. More so than the civilian sector, the absence of an integrated architecture in the past decades was among the leading causes of MTNs heterogeneity. Several deployed communications systems operate, particularly during the conduct of combat. In military tactics, army, air forces, navy, and special units cooperate to obtain specific tactical targets. Different domains employ different types of devices, network structure, offered services and security policies. The ability to provide seamless and adaptive service delivery processes in such a heterogeneous environment is key to the success of next-generation tactical MANETs [16]. In fact, most recent researches have focused on the communication interoperability to capture heterogeneity-enabling technologies. On the other hand, the desire for individual soldiers to always be connected has continued to grow as the underlying technology improves. To accommodate this desire, the Heterogeneous Networks (HetNets) ultimately will become the norm for MTNs as it is for strategic networks and in the Internet.

A. Heterogeneous structure of tactical networking environment.

The next-generation MTNs are evolving into very complex heterogeneous networks in terms of architecture, protocols and security. On the other hand, the systems combine a variety of different transmission technologies (capacity, range, delay, etc.). At a higher level, heterogeneity may also refer to different network policies as well as trust and security management [16]. However, tactical networking structure can be broken into three IT environments. Each of these environments represents a specific group of mission functions. However, all levels together form the multiple operating system environments that need to accomplish assigned tasks. These core types of networks are Strategic level, Tactical deployed lev1e and Tactical mobile level (MTNs) [17]. The heterogeneity problem became more obvious due to variety of technologies, functionality, telecommunications equipment or even nodes mobility at each level. At the highest level, the strategic backbone network with fixed infrastructure provides the high speed and high bandwidth solutions. At the task force, the deployable tactical network with primarily stationary network or satellite system are designed to becoming semi-mobile and adaptable to future missions. At the individual soldier, the high mobility MTNs are characterized by low bandwidth, variable throughput and unreliable connectivity. Therefore, the heterogeneity of tactical scenarios calls for adaptive communication systems that allowing a transparent network for tactical environments, where warfighters can communicate end-to-end without technology boundaries.

B. *Next-Generation architectures solutions for heterogeneity*

The MTNs Advancements for the next generation requires significant improvements to provide greater flexibility and increased interoperability. Services such multimedia content delivery, Blue Force Tracking (BFT) and remote control of sensors will shape tomorrow's digital battlefield environment [18]. Due to the increasing heterogeneity at all levels within military organization, the adoption of software/hardware architecture principles is becoming essential. However, these mechanisms and solutions for the mobile tactical edge must interact very well to meet future Joint Communication requirements. For instance, Joint Tactical Radio System (JTRS) pursued to replace current military MANETs in the USA army with a single set of SDR that can function as multiple radio types and upgrade radio systems with ease. it should be clear that these concepts can enable a broad range of possible outcomes such as ease of spectrum congestion network resources management and dynamic spectrum access for fast network deployment without compromising security [19]. However, the demand will be met by a combination of both tactical and commercial wireless communications techniques. Today gateways or other interconnection techniques are engineered to support tighter integration in large-scale heterogeneous networks [20]. However, the need to increase the reachability and data rate of a wireless network in a tactical environment require the development of new constructs for future network and communication architecture. Instead of using traditional hardware components, an efficient Reconfigurable Radio Systems (RRS) becomes more essential, so that several different ICT systems can be connected. However, table 1 presents a general overview of emerging technologies that need to face and shape the future combat systems [21].

Table 1: **Future trends of tactical heterogeneous solutions**

Novel technologies	**Heterogeneity solutions**
Reconfigurable Radio Systems (RRS)	• Loading the essential waveform and signalling specifications in software. • All technologies for RRS mainly consist of two parts (SDN and CR)

Software Define Networks (SDN)	• The functionality of hardware components provided in software running on a computer or in an embedded system. • Enable the operator to single out the most suitable radio waveform that provide a flexible, widely-applicable solutions for different operating environments
Cognitive Radio (CR)	• Allows intelligent dynamic spectrum allocation to give improved spectral utilization. • Intelligently monitor and analyse its operational radio environment, to decide which frequencies and channels are in use and which are not • Adjust its operational parameters to choose the most appropriate protocols and frequencies for data transmission over wireless channel
Network Functions Virtualization (NFV)	• Decouple network functions from dedicated hardware devices (virtualize), deploy and manage the network service, then • Allow these services to be hosted on virtual machines (VMs). • Build a service chain with less dedicated hardware devices.
IP-based networking	• Enhance connectivity, throughput and backbone network performance with more flexible network configurations. • Offers the prospect of ubiquitous real-time data sharing across different levels of commands and theatre of operations

IV. PHYSICAL- LAYER MODELING

Physical radio link properties are the characteristics associated with the physical link. The tactical network is, however, very different from generic MANETs. For example, the protocols for MTNs must

be tested for highly dynamic topology changes under connectivity characteristics observed in realistic terrains and environments. In practice, the field-tests are time-consuming, costly, and they may not be up to scale. Thus, it is crucial to appoint realistic radio models to investigate performance metrics studies and to gain trust and confidence in the designed MTN. Selecting the appropriate stimulation parameters would underestimate the real performance in the same way as they are implemented on real systems [22]. However, the main models that has a strong impact on the results of the simulation are the movement of the network nodes and the radio wave propagation [23]. This section discusses why most of the mobility models and radio propagation model used in today's commercial MANET simulations are unsuitable to give a good approximation of a military tactical MANET environment.

A. Realistic mobility models of Multi-hop MTNs.

A mobility model plays an important role for evaluation algorithms in MANET. Moreover, the type of movement pattern has a straight effect on the length of the path, link constancy, and size of neighbors for each mobile user. It also intended to capture the routes position, speed, and acceleration change over time. However, there are numerous mobility models [24]. A frequently used Random Waypoint (RWP) for MANET simulations provides the worst-case scenario for protocols performance. in contrast, the movement patterns that their architecture depend on groups/clusters are one of the worst-case scenarios in urban situations [25]. Generally, Simple models draw wrong conclusions of required services the upper layers [26]. The MANET nodes in the commercial applications usually moves in less coordinated way, so the random mobility models are more appropriate in these situations. In contrast, military communications systems tend to require unique solutions. Importantly, in military scenarios, the node movements are influenced by the headquarters or by a mission commander as well as by the tactical goals of the mission. The nodes need to closely collaborate, so their movements are highly correlated. It leads to formation of the mobility groups which are following the mission leader. There is also heterogeneous velocity based on the type of node for either vehicles or pedestrians. In such scenarios where the swarming phenomenon occurs, the group-based mobility model such as Reference Point Group Mobility (RPGM) and Reference Region Group Mobility (RRGM) RPGM model best describes the node movements. However, the provisioning of security in MTNs is more challenging due to nodes mobility and the distributed nature of soldiers make these networks more prone to jamming and eavesdropping.

B. *Realistic Radio Propagation Models of MTNs.*

Another key factor significantly affecting the performance is the choice of the radio propagation model. In fact, it is considered as the most significant factor used as the physical layer models to obtain more accurate and meaningful results [27]. Provided that we assume a radio propagation model that does not accurately describe the realistic propagation conditions, it can either underestimate or overestimate the system performance. The two most important parameters in radio propagation model are the carrier frequency and the transmission distance between the transmitting and receiving antennas. In theory, it used to estimate the transmission power and path loss between nodes for determine the ideal transmission distance. Numerous common numerical models have been developed in the literature with different degrees of complexity and accuracy [28]. In commercial MANETs, network developers commonly offer simple radio that neglect obstacles of the network performance. In the case of tactical MANETs, the mobile propagation paths suffer from several external environmental factors. It is difficult to define a single model that can predict all behaviors of propagation wave. Thus, understanding the effects of varying conditions and awareness of operating area is of vital importance to design mobile LOS tactical network solutions. During the simulation run, tactical planners can evaluate situations and predict of any possible problems that may appear during a real mission. In general, waves that travel through varied terrain and harshest conditions can be described with reflection, diffraction and scattering. Therefore, Two-ray ground propagation model shows better results with varying transmitted power and number of nodes as compared to free space propagation model that using the theory of spreading electromagnetic waves in an ideal vacuum. Moreover, tactical Antenna is a key element in a communication system to suit all operational

requirements. However, this model takes advantages from the physical height of antennas with or without mask [29].

V. PEFORMANCE COMPARISON

NS-2 is used as a simulation tool to evaluate and compare the performance of the of MTN architectures.

A. Comparison Metrics

Four metrics are used to compare the performance of MTNs and MANETs. Here, we assume the following network metrics:

1) Packet delivery ratio: is the average of number of successfully packets received at the soldiers to the total number of packets sent in the network.

2) Routing overhead: to find routes, routing protocols used to send control information (packets).

3) Average throughput: is the ratio of successfully received bits over time needed to transport the bits.

4) End-to-end delay: is the time for packet to reach the destination after leaving the source

B. Network deployment scenario

The current MTNs involve between 20 to 60 nodes which may scale up to 200 nodes in the future designs. The MTNs usually operate in the field of the size, say, 10 by 10 km. The nodes are divided into several groups, and each group has its group leader. One of the group leaders also serves as the main leader of all other groups. The nodes are uniformly distributed about their group leaders who are following the main leader by maintaining a constant distance and the same direction. This yields a mobility pattern that is best described by the reference point group mobility model [30]. The nodes travel at speeds 30-80 km/h, and the mobility is interleaved with pauses of up to 30 min in duration.

C. Simulation Results and Discussion

In this subsection, the performance of MTNs is evaluated

and compared with conventional MANETs. Our simulations assume realistic mobility and radio wave propagation models, as well as the multi-hop capabilities of MTNs. The simulation parameter has shown in Table 2.

Table 2 : **Simulation Parameters**

Object	Parameter	Value
Network node	Medium RF propagation MAC Antenna Routing protocol Number of nodes Packet size Mobility	Wireless channel two-ray ground models 802.11 Omni-directional AODV-HAODV 25-250 512 bytes RWP, RPGM, Manhattan
Network scenario	Simulation time Simulation area size	1000 sec 10 km × 10 km 1 km × 1 km

	Pause time Speed Transmit power	30 sec 80 km/h 46 dBm for vehicles and 30 dBm for patrols

The RPGM and two-ray propagation model describes the physical layer modeling in MTNs more accurately and therefore they are used in this paper. Next, we numerically compare the responses of commercial MANETs and MTNs assuming different protocol type. In this scenario we change the number of nodes. The packet delivery ratio rate for commercial MANETs and MTNs are shown Fig 1. We observe that the HAODV model yields the best performance, and it outperforms the flat AODV protocol considered by 68% on average. In large network, the network can be broken down into a hierarchy of smaller networks, where each level is responsible for its own routing, so cluster-based approaches perform better than flat ones. The average throughput and the average delay for the same set of experiments are then shown in Fig. 2 and Fig. 3, respectively. We can again observe that AODV protocol underestimate the performance of MTNs compared to the performance of more realistic HAODV protocol. The performance bias of different routing protocols is also observed when considering the routing overheads as shown in Fig. 4. The minimum improvement in routing overhead for the HAODV occurred at 25 mobile nodes at which the overhead is decreased by 1.3 compared to AODV, while the maximum improvement occurred at 50 mobile nodes at which the ratio is decreased by 68.9 compared to AODV. On the average, we can realize that the HAODV always outperforms AODV related to minimizing routing overhead at different network densities by 50.8. The key point of H-AODV is that routing scheme can take advantage of hierarchical structure to improve the protocol scalability for large-scale heterogeneous networks.

Military scenarios may be classified by their geographical coverage and the size of the mission. Further, major challenges in MANETs which becomes more difficult when the network size increases. Therefore, the network size is one of the major parameters in simulation studies of routing protocol evaluation in MANET. At the same time, the movement pattern of warfighters can reduce the impact of network area size on the performance of ad hoc routing protocols. Therefore, this study was designed to examine the influence of different kinds of mobility models with varying network size on above-mentioned performance metrics. We consider the following MANET mobility models: RPGM, Random Waypoint (RWP) and Manhattan mobility models. The simulation experimental study has been performed for two different network area sizes of (1000 x 1000 m) and (10000 x 10000 m). This scenario is simulated for 250 number of mobile nodes and two-ray ground model is used for radio propagation model. However, packet delivery ratio at different topology areas size of different mobility models is depicted in Fig. 5. We observe that, the overall performance of the network decreased when the area size is increased. In case of RPGM mobility model the packet delivery ratio decreased by 32% compared in area 1000 m^2. In contrast, RWP and Manhattan mobility model, the performance is very bad when the area size increased, the packet delivery ratio decreased by 64.6% and 74.8% respectively. However, it can be concluded that, the RPGM always outperforms at different operation area size. Fig. 6 compares the average delay and Fig. 7 shows the average throughput results, respectively, for the two simulation area size considered. We observe that, on average, RPGM always outperforms the RWP and Manhattan mobility. In Fig. 8, it has been shown that RPGM is more effective to reduce the route overhead when compared with existing mobility models by 27.4 and 81.4 respectively. Thus, this model is well suited for large operations area with significant barriers to communication (e.g., mountains, oceans, and cities)[14].

VI. Conclusions

When considering the implementation of MANETs in the tactical space for military applications, it is essential to consider the type of transceivers and communication platforms deployed as well as the

application requirements. The unique attributes of MTNs including the specific environment characteristics and deployment scenarios as discussed in this paper have a significant impact on the adoption of MANETs for military use. Thus, assuming generic MANET solutions for the use in military applications can be very misleading in achieving trustable and reliable military grade MTNs.

Despite a vast progress in commercial technologies including ICT, the COTS solutions need to be adapted to the military needs by continuing focused research efforts. The research and development towards enhanced capabilities of MTNs is only as good as the accuracy of the underlying physical models considered, especially considering the mobility and radio propagation models. The MTNs are more demanding to use (often proprietary) protocols to support multi-hop self-forming and self-healing features. Moreover, it is critical to consider the security threats which are often of different nature than in the civilian cyber networks. As the ICT are getting more complex while also becoming the critical part of the communications infrastructures, the use of hardware and software COTS solutions poses severe security risks. The security testing of complex hardware and software components from the 3rd party developers and suppliers is an open and challenging research problem.

Our numerical results confirm the importance of choosing the right models to evaluate the performance of MTNs in order to capture the realistic dynamics of these military networks. We argued that the RGPM model for node mobility and the two-ray model for radio propagation are the most realistic choices to describe the deployment and operation of MTNs. Further investigation was also carried out on the impact of flat protocols and hierarchical routing protocols. The main thrust of the study is to identify a potential hierarchical routing algorithms that much more appropriate for a tactical heterogeneous MANET topology. Such behavior was observed generally for all the performance metrics considered. The last numerical results in the paper illustrate the influence of different operation area sizes on network performance under different mobility patterns. The result shows that how environmental parameters such as the size of operation play central role to determine the network properties that are more accurate, especially in large operations area, such as disaster area recovery, urban warfare and reconnaissance. Also, the increase in area size can have a significant impact on network performance and reliability. High network density can improve the network performance in terms of reliability and robustness. However, it caused many challenges in the design management of military MANETs. Finally, the outcomes are very useful to present the importance of using realistic simulation environment in order to compare and assess the performance of different technologies used in the tactical network.

Bibliography

[1.] Fossa, C. and T. Macdonald. Internetworking tactical manets. in MILITARY COMMUNICATIONS CONFERENCE, 2010-MILCOM 2010. 2010: IEEE.

[2.] Board, N.S. and N.R. Council, C4ISR for future naval strike groups. 2006: National Academies Press.

[3.] Wang, H., et al. Implementing mobile ad hoc networking (MANET) over legacy tactical radio links. in Military Communications Conference, 2007. MILCOM 2007. IEEE. 2007: IEEE.

[4.] Thompson, B. and R. Harang, Identifying key cyber-physical terrain (extended version). arXiv preprint arXiv:1701.07331, 2017.

[5.] Tortonesi, M., et al., Enabling the deployment of COTS applications in tactical edge networks. IEEE Communications Magazine, 2013. 51(10): p. 66-73.

[6.] Agre, J.R., K.D. Gordon, and M.S. Vassiliou, Commercial technology at the tactical edge. 2013, INSTITUTE FOR DEFENSE ANALYSES ALEXANDRIA VA.

[7.] Larsen, E., TCP in MANETs–challenges and Solutions. FFI-Rapport-2012/01514, 2012.

[8.] Elmasry, G.F., Tactical wireless communications and networks: design concepts and challenges. 2012: John Wiley & Sons.

[9.] Koch, R. and G.D. Rodosek. The role of COTS products for high security systems. in Cyber Conflict (CYCON), 2012 4th International Conference on. 2012: IEEE.

[10.] Zheng, D.E. and W.A. Carter, Leveraging the internet of things for a more efficient and effective military. 2015: Rowman & Littlefield.

[11.] Burbank, J.L. and W.T. Kasch. COTS communications technologies for DoD applications: challenges and limitations. in Military Communications Conference, 2004. MILCOM 2004. 2004 IEEE. 2004: IEEE.

[12.] Marsden, S. and J. Vankka, Providing a tactical domain for an independent nations task force. 2015.

[13.] Vassiliou, M.S., D.S. Alberts, and J.R. Agre, C2 Re-envisioned: The Future of the Enterprise. 2014: CRC Press.

[14.] Al-Shehri, S.M., et al. Comparing tactical and commercial MANETs design strategies and performance evaluations. in Military Communications Conference (MILCOM), MILCOM 2017-2017 IEEE. 2017: IEEE.

[15.] Chan, V., et al., Future heterogeneous networks. 2011.

[16.] Hauge, M., et al., Selected issues of qos provision in heterogenous military networks. International Journal of Electronics and Telecommunications, 2014. 60(1): p. 1-7.

[17.] Kärkkäinen, A., Developing cyber security architecture for military networks using cognitive networking. 2015.

[18.] Seddar, J., et al. Exploiting cognitive radios in tactical point to multipoint communications. in Military Communications and Information Systems Conference (MCC), 2013. 2013: IEEE.

[19.] Tang, H. and S. Watson, Cognitive radio networks for tactical wireless communications. 2014, Defence Research and Development Canada-Ottawa Research Centre Ottawa, Ontario Canada.

[20.] Bernier;, F., et al., C2 in Underdeveloped, Degraded and Denied Operational Environment, in 18th ICCRTS. 2013: U.S.A.

[21.] Sigholm, J., Secure Tactical Communications for Inter-Organizational Collaboration: The Role of Emerging Information and Communications Technology, Privacy Issues, and Cyber Threats on the Digital Battlefield. 2016, Högskolan i Skövde (University of Skövde).

[22.] Reidt, S., Efficient, Reliable and Secure Distributed Protocols for MANETs. 2010.

[23.] Gunes, M. and M. Wenig. On the way to a more realistic simulation environment for mobile ad-hoc networks. in International Workshop on Mobile Services and Personalized Environments, GI LNI. 2006.

[24.] Chaturvedi, A.K. and J.K. Khemani, Analysis of Mobility Models in Mobile Ad-hoc Networks. International Journal of Computer Applications, 2014: p. 5-9.

[25.] Zhang, H., et al., Mobile Ad-Hoc and Sensor Networks: Third International Conference, MSN 2007 Beijing, China, December 12-14, 2007 Proceedings. Vol. 4864. 2007: Springer.

[26.] Dricot, J.-M. and P. De Doncker. High-accuracy physical layer model for wireless network simulations in NS-2. in Wireless Ad-Hoc Networks, 2004 International Workshop on. 2004: IEEE.

[27.] Basagni, S., et al., Mobile Ad Hoc networking: the cutting edge directions. Vol. 35. 2013: John Wiley & Sons.

[28.] Eltahir, I.K. The impact of different radio propagation models for mobile ad hoc networks (MANET) in urban area environment. in Wireless Broadband and Ultra Wideband Communications, 2007. AusWireless 2007. The 2nd International Conference on. 2007: IEEE.

[29.] Burbank, J.L., W. Kasch, and J. Ward, An introduction to network modeling and simulation for the practicing engineer. Vol. 5. 2011: John Wiley & Sons.

[30.] Li, L., et al., Network properties of mobile tactical scenarios. Wireless Communications and Mobile Computing, 2014. 14(14): p. 1420-1434.

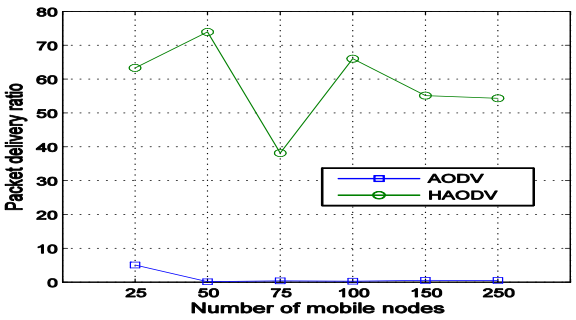

Figure 1: **Packet delivery ratio under different network density**

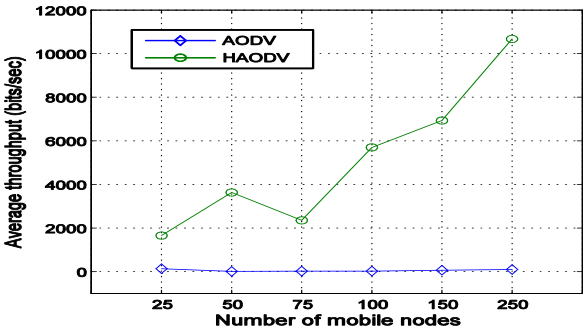

Figure 2: **Average throughput under different network density**

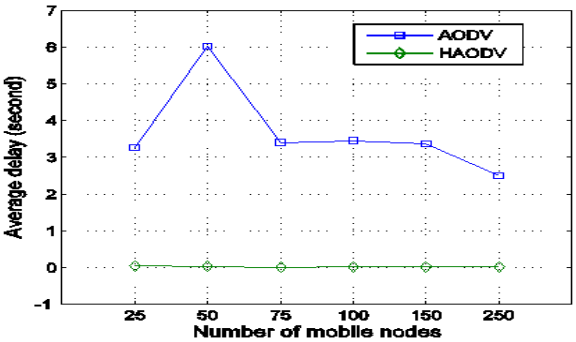

Figure 3 : **Average delay under different network density**

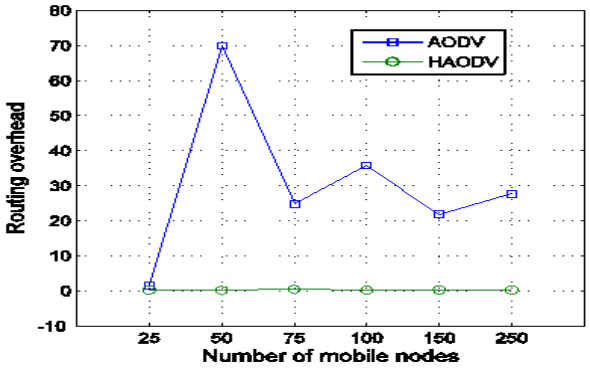

Figure 4 : **Routing overhead under different network density**

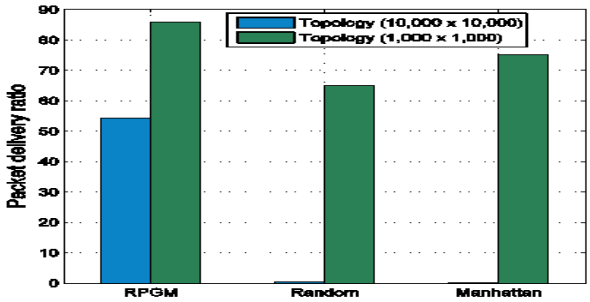

Figure 5: **Packet delivery ratio under different topology area**

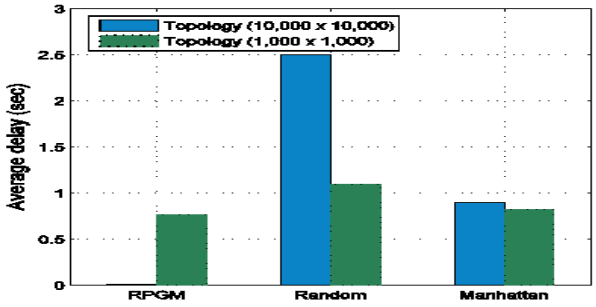

Figure 6: **Average delay under different topology area**

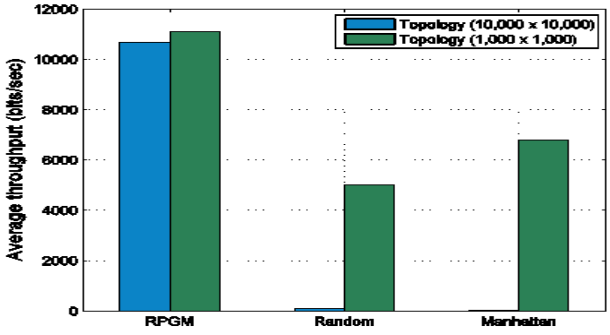

Figure 7: **Average throughput under different topology area**

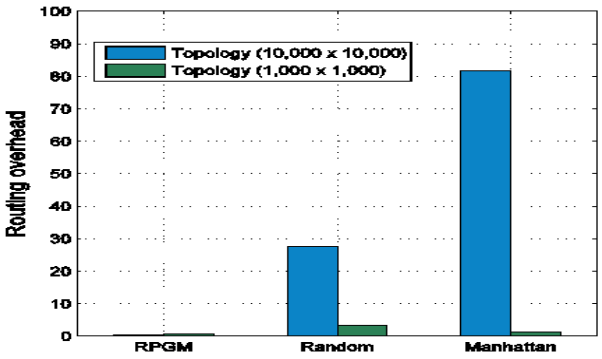

Figure 8: **Routing overhead under different topology area**